Functional brain networks constructed in subjects' native spaces

Emanuele Sicurella

School of Science

Thesis submitted for examination for the degree of Master of Science in Computer, Communication and Information Sciences

Espoo 30.07.2018

Supervisor

Prof. Jari Saramäki

Advisor

Dr. Onerva Korhonen

Aalto University
School of Science

Aalto University, P.O. BOX 11000, 00076 AALTO
www.aalto.fi
Abstract of the master's thesis

Author Emanuele Sicurella

Title Functional brain networks constructed in subjects' native spaces

Degree Programme MSc. Computer, Communication and Information Science.

Major Computer Science

Supervisor Prof. Jari Saramäki

Advisor Dr. Onerva Korhonen

Date 30.07.2018 **Number of pages** 65 **Language** English

Abstract

Due to the structure of the human brain and its functioning, it can be modelized as a network, i.e. a collection of nodes connected by links. One of the approaches consists in constructing functional brain networks, where nodes are identified by regions of interest (ROIs) composed of neurons with similar functional activation.

The main issue of this kind of approaches is how to define nodes and links. In a typical functional brain network construction pipeline, one critical step is the registration of brain areas into templates which makes possible statistical analysis and comparison across different subjects and studies.

Different registration methods can lead to different results.

Here, we compare standard space registration method with a new method, called inverse-registration, starting from raw data provided by functional Magnetic Resonance Imaging (fMRI).

In standard registration, data is projected into a standard common space, which is the same across different subjects and studies. In inverse registration approach, a template from Standard space is (inverse) registered to structural space and the obtained images are finally registered to the functional subject space. We found out that inverse registration leads to nodes with increased functional homogeneity, while basic network properties are not significantly affected.

These results suggest that inverse registration is a better registration method, although it is very recent and further investigation is needed before generalizing this statement.

Keywords Brain Networks, Computational Neuroscience, Inverse Registration, ROIs, Functional Homogeneity

Contents

Chapter 1

Introduction

1.1 Complex Systems

Since its birth, science, physics in particular, has been claimed to have a strictly deterministic character. Although the intervention of quantum mechanics has strongly outlined the inevitable presence of uncertainty in nature, it remains to be asked whether indeed any macroscopic system, away from microscopic bizarreness, can be predictable in a deterministic way.

For a physicist, all the properties of a system are contained in an equation: a law enunciated in mathematical language whose solution at any given moment describes exactly how the properties of the initial system evolve in time. However, we are now aware of the fact that some systems composed by many interacting bodies have not an analytical solution because they are described by equations that can be solved only with numerical methods. Components of this kind of systems interact nonlinearly and hence, it is extremely difficult (or even impossible) to predict their future evolution, although they are deterministic systems [1].

Of course the presence of many bodies is not the only requirement to have this kind of behaviour. Perfect gases, for example, have a number of microscopic components in the order of 10^{23} which interact in a very complicated way, but in spite of that the macroscopic behavior is predictable and described by simple parameters. In such cases, instead of writing 10^{23} equations of motion we use the approach of statistical mechanics. **Statistical Mechanics** describes those systems using macroscopic parameters such as temperature, pressure, etc [2].

The systems described above can also be studied with tools from Statistical Mechanics. However, they are neither predictable nor chaotic systems: they are about halfway in correspondence to what is called the *edge of chaos*. Such systems are called **Complex Systems** and they can be found in Physics or even in Biology, Sociology and Economics. One interesting property is that the evolution of a system like this can lead to what is called **emergent phenomena**, a macroscopic (global) result that is in no way predictable by the interaction of the individual elements [1].

Taken the fact that complex systems are composed of many interacting bodies, it is natural to model them as a network, *i.e.* a collection of **nodes** which are connected with **links** [3]. The most interesting thing is that the structures of very different kind of complex systems show same patterns and properties suggesting us that some fundamental principles should exists. Consequently, those systems, no matter what their nature is, can be analyzed using a common set of mathematical tools: the WWW where nodes are the pages of a website and the links are the hyperlinks between pages or sites, socio-economic networks (online or offline) where nodes are people, banks or enterprises and links are friendship or professional relationships, biological networks like metabolic networks, genes network and, of course, neuronal networks. The field that studies these different networks, as well as their abstract theoritical model, is called Network Science. Its aim is to extract knowledge from these systems to better understand their structures and dynamics.

1.1.1 The Brain as a Complex System

The human brain's activity is basically due to neurons, electrically excitable cells that exchange electrical and chemical signals through connections called **synapses**. The average adult human brain contains around 86 billions of neurons [4]. Each of the 86 billions neurons has on average 7,000 synaptic connections to other neurons. It has been estimated that the brain of a three-year-old child has about 10^{15} synapses while for an adult, the numbers range from 10^{14} to $5 \cdot 10^{14}$ [5].

Looking at those numbers seem reasonable to define the human brain as a complex system. Several studies have observed many properties of complex systems in the brain, for example non-linearity [6] or self-organized criticality [7].

1.2 The Brain as a Complex Network

As described above, neural systems are based on interactions in the form of electrical and chemical signals so they can be easily modelled as a network. The field that studies this systems using the network-oriented tools is called network neuroscience.

But how exactly can the brain be modeled as a network? The first intuitive approach would be imagine neurons as nodes and synapses as links. Unfortunately, this method has two major problems:

1. As said, the number of neurons and synapses is huge. Therefore, a simulation of a full human brain would require a computational tecnology far better than the one we actually possess. To make a comparison, the only neural system analyzed at single neuron and synapse level is the nervous system of the nematode worm Caenorhabditis elegans, which consists in 2,287 synapses connecting 279 neurons [8]. Also imaging methods with such resolution are still missing.

2. Even if it is possible to create a perfect full-scale replica of a human brain, the model would be as complex as the original system and it would be hard to extract knowledge from it.

Anyway, the brain posses a particular structure of groups of strongly connected neurons specialized on the same task [9, 10]. This enables focusing only on some of these areas or studying the whole brain at a larger scale analyzing the interections between these areas. However, choosing the right brain area to identify as node is not only question of numbers of neurons involved. Indeed, brain networks are commonly divided into three categories [11]:

1. **Structural networks.** This is maybe the first intuitive approach (and also the historically oldest). In structural networks, brain areas are anatomical portions of the brain tissue which are physically connected by white matter tracks.

2. **Functional networks.** Here, links are identified in terms of some similarity measure which determines how strong is a connection, *i.e.* temporal coactivation. In this kind of networks, links might not represent interactions between areas.

3. **Effective networks.** Also here, the same nodes are used, while links represent the influence of a brain area to another. Hence, links always represent interaction.

In this thesis, functional networks from data acquired with functional magnetic resonance, or fMRI (see 3.1), are utilized. Data is based on 4-dimensional images (where time is the 4th dimension) composed by a collection of volumes, called voxels, the intensity of which represents activity.

One more issue is that there is no single size that would be optimal for brain regions used as nodes of functional brain networks. Hence, brain networks have been studied at very different range of scales: from whole brain networks compound of 70 nodes [12] to 140,000 nodes [13]. This could be an opportunity because network model can be constructed differently based on the requirements of each study [14], but also a threat, because the number of the nodes significatly affects network properties [12].

1.2.1 Network Neuroscience

Studying the structure and connections in the brain, human and animal, has been a common approach since long time ago [15]. For examplex, the first method to identify brain areas was post-mortem histology, i.e. histological analysis of the brain in order to physically find boundaries which should have identified the areas boundaries [16]. However, it is in the beginning of 1980's that computational models started to change completely this kind of research. Since then, a lot of studies used computational models to combine mathematical results on anatomy (connection matrix) and physiology (biophysical processes) [17]. Several interesting results have been achieved since then, like the observation of emergent rhythmicity [18] or syncronization among neural populations [19].

Brain research interest exploded around mid-1990's, when non-invasive imaging tecniques were developed [20]. Since then, data has grown exponentially both in number of samples and in complexity (for example, capturing larger portions of nervous systems) [21]. Today, most of these big data are in form of networks [22], representing protein interactions, neural systems with synaptic connections or interactions between whole brain systems [23] and even social networks [22].

Baically, the research was first conducted on structural networks and then continued on functional networks. Starting from the early 21st century, the

concept of connectome, the structural description of the brain that can be studied with network science, has been introduced [24] and methods from network science were, for the first time, applied to the analysis of experimental neuro-imaging data [25]. The developing of new methods and tools in computer science and network science, as well as the growing amount of data, lead authors to define a new discipline, called network neuroscience [26].

Network neuroscience is a new discipline but already achieved important results. For example it was outlined the presence of hubs in the brain, *i.e.* higly connected nodes which can be crucial for information transfer and processing [26, 27, 93]. It was observed that in the brain, hubs tend to be strongly connected each other in what are called rich clubs [29]. Furthermore, the other nodes, which form the perifery, are connected to the hubs which are found in the center. This property is called core-periphery organization [29] (this concept should not be confounded with the concept of assortativity, which measure the tendency of similar-degree nodes to connect each others, see 2.2.4 for details). A more global results tells us that brain is organized in hierarchical communities, i.e. strongly connected subnetworks which can be further divided into smaller communities [29]. It was also observed that brain structure changes with age or because neurological deseases such as Alzheimer's or autism spectrum disorder and this could be crucial in order to find a remediation for those illnesses [30, 31].

Network Neuroscience has been focusing on static networks, but one of the main challenges is represented by the study of dynamic networks, *i.e.* networks that may change their structures in time [22]. Furthermore, more interest will be put in dynamic prediction of networks and effects of perturbation and manipulation in order to control the specific output of the system [22].

1.2.2 The Non-Trivial Problem of Defining Nodes

Focusing on functional brain networks, is crucial to choice the boundaries of nodes and this can influences the result of the study in several ways [32]. Actually, there are three mainly used approaches for defing nodes in functional networks [33]:

1. **Voxel-Wise Approach.** Each individual voxel is identified as a node. In this way, nodes have the same dimensions. Number of nodes can

vary widely across different studies, from 3,400 nodes [34] to 140,000 [13].

2. **Structural Anatomical Atlases.** Nodes are particular Regions-of-Interest (ROIs) identified starting from a readily available structural anatomical image which works as a template (atlas). In each of these areas, fMRI average signal for all of the ROIs into that area is calculated and used for defining links [33].

3. **Functional Activation Meta-Analytic Approaches.** Nodes are defined by analyzing previous fMRI studies in order to find a set of fixed ROIs that will be used for all of the following similar studies. They are modeled as 3-6 mm radii spheres which center is a point of maximum activity in functional area [35, 36].

Although some authors recommends voxel-wise approach [33], the method used in the major part of the studies is the structural anatomical atlases approach, and it's the one that has been used in order to create the data for this study.

The main advantage is that with this approach, it is possible to register atlases into a standard space during preprocessing, and that is useful to have a universal comparison standard across subjects or even different studies [37]. However, weak points are present, too. The main critique to this approach, is about the coarse resolution (number of ROIs is typically from 70 to 250). This may cause some brain areas, with different functions, to collapse into a single node [38]. Hence, a network constructed in this way may not be a good model of real brain because it may show different properties from the ones of networks constructed in other ways. This problem was outlined by calculating the ROI functional homogeneity, a certain measure of similarity between components time series within a ROI [39], and showing that it is very poor [33, 40].

The poor ROIs functional homogeneity is clearly a main issue that has to be take into account. Recently, a new way to register atlases has been developed in order to try to solve this issue. The idea is that, instead of registering atlases in a common standard space, each ROI is "inverse" registered into the correspondent subject native space. So, even if the ROIs are still big, they will take into account anatomical variation between subjects. This method is called inverse registration and its valitadion is the main goal of this thesis.

1.3 Structure of the Thesis

The aim of this work is to apply network-oriented tools to validate the inverse-registration method for constructing brain networks from fMRI data.

The thesis is divided in two parts: part 1 is about the theoretical background. In chapter 2, I will first present in detail network science theory defining some basic measuress that will be used to make a comparison between networks with inverse-registered nodes and registration in standard space. In chapter 3, I will describe the complete procedures of obtaining brain networks. First of all, data has to be acquired. In this study, MRI and fMRI are used in order to obtain respectively structural high-resolution images and functional low-resolution images; I will explain briefly these tecnique (which also are a nice example of the application of Physics to Biology). Then, nodes and links have to be defined; this is the main problem of my thesis (and also one of the main problems in Network Neuroscience in general) and I will explain in detail how this goal can be reached. Finally, I will explain in detail the registration in standard space and inverse-registration approaches for defining nodes of brain networks. It will be important to outline the main differences in terms of pros and cons.

Part 2 is the practical part of the thesis. In chapter 4, I will present the matherials and methods, *i.e.* the theoretical and practical tools that will be used to pursue the aim of this study. This chapter contains the information about how dataset and subjects have been selected, methods for constructing nodes and links, and methods and tools that have been used to analyze brain networks. In chapter 5, I will present the results of the study. I will calculate the spatial consistency of the nodes in both networks, *i.e.* how much the nodes are correlated each others, and make a comparison. Indeed, the central goal of this research is to see if inverse-registered network nodes have a higher spatial consistency. This will prove that back-registration is a better method to define nodes than the ones utilized until now. Further, I will compare networks constructed with two different node-definition strategies in term of some network properties (explained in chapter 2) to eventually spot relevant differences. In chapter 6 I will briefly discuss the results at a general level. I will also talk about limitations and possible further research.

Part I

Theoretical Background

Chapter 2

Network Science Tools

We said that interaction is a fundamental feature of complex system, and know how components interacts each other is fundamental if we want to exctract knowledge from those systems. In order to do this, in this chapter I will describe the fundamentals of Network Science. The informations in this chapter are retrieved from [41], if not differently specified.

2.1 Graphs and Networks

We will call these components **nodes** or **vertices** and the interactions **links** or **edges**. This representation is well suited for studying systems whose nature is totally different. Such representation, which doesn't take into account the nature of the network, but only its structure, is called **graph**.

Graphs or networks have two basic parameters:

1. N, the number of nodes or vertices. It is also called the size of the graph or network. Different nodes are labeled with an index $i = 1, 2, ..., N$.

2. L, the total number of links or edges. Links are usually identified through the nodes they connect. For example (1, 4) means that there is a link connecting nodes 1 and 4.

The links of a network can be *directed* or *undirected*. Directed links lead information or interaction only in a single way: for example, a URL in the WWW points from one resource to another, and not vice versa. Undirected links work in both ways: for example in social networks if A is a friend of

B, normally B is a friend of A. The same network may have both undirected and directed links, for example in metabolic networks where certain proteins interactions may be irreversibile (directed links) while others reversible (undirected links). A network is called directed if it only contains directed links; it is called undirected if it only contains undirected links. In this work, we will focus on undirected networks (see 4.2.2 for details about the links definition used in this work).

2.1.1 Adjacency Matrix

To obtain a complete description of a network, we need to have a complete information about all of its links. The easiest representation of all of the links is in the form of a matrix. This matrix is called **adjacency matrix,** and for a network with N nodes, it is a $N \times N$ matrix whose elements are:

$$\begin{cases} A_{ij} = 1, \text{ if there is a link pointing from node j to node i} \\ A_{ij} = 0, \text{ if nodes } i \text{ and } j \text{ are not connected each other} \end{cases} \tag{2.1}$$

In an undirected network $A_{ij} = A_{ji}$, *i.e.* the adjacency matrix is symmetric.

2.2 Network Properties

We will see now some of the most important measuress used in network science which can tell us a lot of information about the network we are studying.

2.2.1 Degree and Degree Distribution

The **node degree** is defined as the number of links the node has with other nodes. We denote with k_i the degree of the i^{th} node in the network. For an undirected network the total number of links, L, is the sum of the node degrees:

$$L = \frac{1}{2} \sum_{i=1}^{N} k_i \tag{2.2}$$

The $\frac{1}{2}$ factor is a correction because in the sum, each link is counted twice.

An important measure which characterize different properties in networks is the **degree distribution**. The degree distribution, p_k, is the distribution

of the probability that picking a random node in the network it has degree k, and of course it must be normalized:

$$\sum_{k=1}^{\infty} p_k = 1 \tag{2.3}$$

For a network with N nodes the degree distribution is represented by the normalized histogram:

$$p_k = \frac{N_k}{N} \tag{2.4}$$

where N_k is the number of degree-k nodes. It can be derived from the degree distribution as $N_k = Np_k$.

If we know the adjacency matrix, we can easily caluate the degree k_i of node i. In order to do this, for undirected networks, we sum over the rows or the columns of the matrix, obtaining the same result:

$$k_i = \sum_{j=1}^{N} A_{ji} = \sum_{i=1}^{N} A_{ji} \tag{2.5}$$

2.2.2 Clustering Coefficient

Node clustering coefficient tells us how connected local neighborhoods of the node are. The definition of local clustering coefficient for a node k_i is [42]:

$$C_i = \frac{2L_i}{k_i(k_i - 1)} \tag{2.6}$$

where L_i is the number of links between the k_i neighbors of node i. This coefficient vary between 0 (none of the neighbors of node i link to each other) to 1 (the neighbors of node i form a complete graph, *i.e.* they all link to each other) and is basically the measure of the probability that two neighbors of a node link to each other.

It is possible to define the average clustering coefficient:

$$\langle C \rangle = \frac{1}{N} \sum_{i=1}^{N} C_i \tag{2.7}$$

i.e. the average of C_i over all nodes $i = 1, ..., N$. In probabilistic terms, $\langle C \rangle$ is the probability that two randomly picked neighbors of a determined node link to each other.

It is also interesting to ask ourselves how the local clustering coefficient varies with node degree. In order to do this, we define a function:

$$C(k) = \frac{1}{N_k} \sum_{j=1}^{N_k} C_j \tag{2.8}$$

where we refer as node degree with k instead of k_i because we are no longer interested in single nodes, but rather in degrees. This function calculate the average clustering coefficient over all nodes with the same degree k.

The coefficients calcuated in 2.6, 2.7 and 2.8 refer to unweighted networks. Generalize the concept of clustering coefficient for weighted network is possible, but not trivial. Indeed, there are many different weighted clustering coefficient each leading to different results and behaviors [43]. For this reason, in this work we will focus only on unweighted clustering coefficient.

2.2.3 Shortest Path

In Physics, physical distance is usually essential to determine the properties of interactions. However, in networks, what matters is the distance between two nodes which is expressed by **path lengh**, *i.e.* the number of links the path contains. The most important is usually the shortest path. The shortest path between nodes i and j is the path with the fewest number of links. This is often called distance between i and j and represented as d_{ij}. The distance between the two most distant nodes in the network is called the longest shortest path d or diameter of the network.

2.2.4 Assortativity

Observing real networks, it could be found that nodes tend to have a spefic behavior about connection with similar-degree node. For example, very high-degree nodes, called hubs, can prefer to connect with other hubs, or conversely, try to avoid them. We can define two kinds of real networks depending on this behaviour:

Assortative In these networks, nodes tend to connect to ones with a similar degree. Hence, hubs tend to connect with other hubs and avoid low-degree nodes.

Disassortative the hubs avoid each other, linking instead to low-degree nodes.

A quantitative way to define this property is the use of a degree correlation matrix, e_{ij}, where each element represents the probability that a randomly picked link connects nodes with degrees i and j. Since e_{ij} is a probability, it must be normalized:

$$\sum_{i,j} e_{ij} = 1 \tag{2.9}$$

Even if all the information about degree correlation is contained into e_{ij}, it is difficult to extract information from the visual inspection of the matrix. Moreover, it is difficult to compare networks with different correlations. For those reasons, it is useful to define an assortativity coefficient [44]. This allows us to define assortativity using only one number. The assortativity coefficient is defined as the mean Pearson correlation coefficient between the degrees of the nodes connected by a link, where the average is done across all connected nodes pair. Its values range between $-1 \leq r \leq 1$. Negative values indicate disassortativity, and positive values assortativity.

Assortative networks The fact that in assortative networks hubs tend to connect each other is reflected by the fact that the correlation is positive. Hence, $0 < r \leq 1$. This is the case for example for social networks.

Disassortative networks In disassortative networks, the correlation is negative, hence $-1 \leq r < 0$. This is the case of metabolic networks.

Neutral networks In neutral networks, nodes link to each other randomly. Hence there no correlation in the linking pattern and $r = 0$.

2.2.5 Weighted Networks

So far we have assumed that links have the same weight but in many real cases, different links may have different relevance. Networks with those kind of links are called weighted networks (for a complete analysis of weighted networks, see [43]). In this case, adjacency matrix elements represent the weight of the link:

$$A_{ij} = w_{ij} \tag{2.10}$$

Many of the real networks are weighted, but determining link weight is not always trivial. Consequently, we often approximate these networks with an unweighted graph. Sometimes it is easier to calculate some unweighted network parameters even for weighted networks. In order to do this, we may consider a thresholded network, *i.e.* a network where we keep only a certain percentage of the strongest link and forget about the others. We assign then to the strongest links a weight 1 and consequently trasforming it into an unweighted network. Thresholding is also useful when we have full matrices that we want to transform into a network.

Node Strength

We can generalize the notion of degree for weighted network by defining node strength as follow:

$$S_i = \sum_{j=1}^{N} w_{ij} \tag{2.11}$$

2.3 Different Types of Networks

2.3.1 Scale-free Networks

One can intuitively think that degree distribution in networks is symmetric, *i.e.* there will be equally low degree and high degree nodes, but the most part of the nodes will lay into a medium degree region. This is actually true for random networks, *i.e.* networks constructed by assigning a certain number of links randomly between nodes. In random networks, node degree distribution follows a Poisson distribution [45]. Anyway, if we compare it with degree distributions of real networks, there are a lot of differences. That means that real networks are very far from random networks.

Degree distribution of real networks are often well approximated with a power law distribution defined as follow [45]:

$$p_k \sim k^{-\gamma} \tag{2.12}$$

where γ is the degree exponent. If we take a logarithm of 2.12, we obtain:

$$\log p_k = -\gamma \log k \tag{2.13}$$

So, $\log p_k$ depends linearly on $\log k$ with slope γ.

The main consequence of a network following this distribution is the presence of hyper-connected nodes, *i.e.* nodes with very high degree or hubs.

2.3.2 Small-World Networks

The small-world phenomenon states that given any pair of nodes in a network, their distance is much smaller in comparison of the dimension of the network [42]. In mathematical terms, it can be found that the small-world property can be expressed as follow:

$$d_{max} \approx \frac{\log N}{\log \langle k \rangle}, \tag{2.14}$$

where d_{max} is the distance between the two most distant nodes, N is the dimension of the network and $\langle k \rangle$ is the average degree. Hence, the maximum distance is proprotional to $logN << N$ for high values of N.

Although random networks possess the small-world properties, in order to define small-work networks, also another requirement should be satisfied [42]. The average clustering coefficient in small-world networks is higher than the one expected for a random network of similar dimension and number of links. A mathematical way to state this is that:

$$\frac{\langle C_{sw} \rangle}{\langle C_{rnd} \rangle} > 1, \tag{2.15}$$

where $\langle C \rangle$ is the average clustering coefficient.

Chapter 3

Constructing Brain Networks

In this chapter, I will describe in detail the full path that brings us from getting an image of the brain to the construction of the network that can be analyzed with network science tools described in chapter 2.

3.1 Data Acquisition

The first step is obtaining an image of the brain and many tecniques can be used. A well-known method for studying the brain is fMRI or functional magnetic resonance imaging. This is a non-invasive method that consists on using magnetic resonance imaging (MRI) to evaluate the functionality of an organ or apparatus.

3.1.1 Magnetic Resonance Imaging (MRI)

MRI is based on nuclear magnetic resonance (NMR) phenomenon. It consists in applying a strong static magnetic field, usually of 3T, to the patient. This causes spin of tissues' protons to align with the magnetic field in parallel (majority) or antiparallel [46, 47]. In classical systems (which are a good approximation of quantum macroscopic system with spin 1/2), spin of atomic nucleus are described with a vector $\overrightarrow{\mu}$ called magnetic moment. In this case, there will be a small positive total magnetization $\overrightarrow{M}$, defined as the vectorial sum of the nuclei's spins$\overrightarrow{\mu}$ [46, 47]. To observe $\overrightarrow{M}$, we have to perturbate the system, and this can be done by the application of a short magnetic pulse B_1 called excitatory field (B_0 is called polarization field). This causes

$\overrightarrow{M}$ to rotate and, when the effect of the excitatory field is over, it slowly returns to the equilibrium where the net magnetization again aligns with the polarization field [46]. The system gives back the excess of energy by emitting a radio pulse that can be recorded [47]. The NMR signal, called FID (free induction decay), is roughly monochrome and attenuating exponentially as a function of the relaxation time, *i.e.* the length of the time required for returning to the equilibrium state. This time, and therefore the duration of the radio wave, depends on the concentration of hydrogen atoms (proton nuclei) in the tissue [47].

For brain imaging in particular, measures are taken in sequence of overlaying layers until the whole head is covered. Every layer is a 2D image which is divided in pixels. Each pixel has a particular intensity, which is proportional to the correspondent relaxation time. Finally, the layers can be combined to generate a three-dimensional image of the head. Overlaying pixel, a 3D basic unit, called voxel, is generated. A voxel is a three-dimensional cube with edge length of 2–8mm, each one containing on average 5.5 millions of neurons [47]. This is an excelent resolution but we should keep in mind that it is clearly far from the neural level.

3.1.2 Functional Magnetic Resonance Imaging (fMRI)

While MRI is useful for medical diagnostic because it gives us a static image of the structure of the brain, a temporal dimension is necessary to observe the function of the brain. Functional magnetic resonance imaging (fMRI) is the method used in order to reach this goal [48]. In fMRI, a sequence of magnetic pulses, instead of a single one, is applied to the brain and then, the temporal evolution of the relaxation times is measured. As said in the previous section, relaxation time depends on the properties of the tissue. The frequency of the pulses, which is called repetion time (TR), provides the temporal resolution of fMRI. TR is influenced by spatial resolution: the more slices collected (more spatial resolution), the longer TR is required. TRs of approximately 2 seconds are typically used.

BOLD signal

Adding a temporal resolution is not sufficient for studying the function of the brain: MRI is based on nuclei magnetic properties which of course depend

on the tissue but not on its functionality. In order to solve this problem, fMRI uses the magnetic properties of hemoglobin molecule in blood.

The idea is that because cell metabolism requires more oxygen, which is carried by hemoglobin, more oxygenated blood in a brain area means that this area is more active [49]. Deoxygenated hemoglobin (dHb), *i.e.* hemoglobin without oxygen bound, possess a spin excess (paramagnetic), while oxygenated hemoglobin (Hb) is neutral. This difference causes a drop in the measured MRI signal [47, 49, 50]. Blood-oxygen-level dependent (BOLD) signal is a signal correlated to the change in the ratio between oxygenated and deoxygenated hemoglobin. Measuring BOLD signal for each voxel gives us a time series of three-dimensional brain images (volumes).

However, the use of BOLD signal to identify more active brain areas presents some issues. First of all, fMRI BOLD is not a direct measure of brain activity because changes in neuronal activity are not immediatly traduced in BOLD signal. Increase in blood flow because of neuronal activity, known as neurovascular coupling, is not a simple mechanism and requires several seconds to be observable in terms of BOLD signal. This, of course, affects the temporal resolution of fMRI [50]. Moreover, BOLD signal may change across subjects or even in the same subject at different times and it is affected by physiological factors, like smoking, alcohol or drugs consumption and physical exercise [47].

3.2 Preprocessing

The acquired raw data is not ready for being analyzed. Indeed, we need to make sure the signal from each voxel contains the right temporal and spatial information. In order to do this, it is usually necessary to make some adjustments in the phase of preprocessing.

The first step is usally to correct head motion of the patient. Motion will result in a mismatch of the location of subsequent images in the time-series and this is translated in higher noise. This type of motion problem, however, usually corresponds to wholesale movements (bulk-motion) and is well corrected by rigid transformations [52].

Another correction that may be applied is the temporal filtering [51]. It aims to reduce or completely remove undesired frequencies within the raw signal, provoqued for example from cardiac pulses, respiration or general noise due to the scanner. This can improve SNR but the right frequencies to

discard have to be identified, *e.g.* if for fMRI TR is 2 seconds, then we want to keep frequency around 0.5 Hz.

One very important step of preprocessing is normalization. It aim is to project subjects' brain images to a standard space in order to make easy the comparison between those images. The process is explained in detail in 3.5.

3.2.1 Spatial Smoothing

Spatial smoothing is a typical preprocessing procedure which aims to reduce the differences between near voxels in order to reduce the effects of noise [39]. This can be done by averaging each voxel's time series with the ones of their neighbours. Each neighbour voxel's time series is weighted using a smoothing kernel, typically Gaussian:

$$x_i = \frac{\sum_j G_i(j) x_j}{\sum_j Gi(j)}, \tag{3.1}$$

where x_i is the time series of voxel i, $G_i(j)$ is the smoothing kernel value at voxel j, but centered at voxel i. Kernel is defined in terms of FWHM (full width at half maximum) which identifies the distance (in mm) at which the filter is applied and hence, the the extent of smoothing.

So, spatial smoothing increases the signal-to-noise (SNR) ratio, but also reduces spatial resolution and hence, a good balance has to be found between improving SNR and maintening an accetable image resolution [39]. Furthermore, many other negative effects have been reported for the use of spatial smoothing, in the structures and properties of networks, and for these reasons its use in this kind of research is controversial [39]. For these reason, spatial smoothing has not been applied to the data used in this study.

3.3 Parcellating the Brain

After images acquisition, the following step is defining what a node is and how to obtain it from images in order to proceed to the preprocessing phase (although all preprocessing is typically done *a priori*, for comodity the whole preprocessing phase is explained in 3.2). As discussed in 1.2.2, identifying nodes in brain networks is a central problem so the problem has to be approached carefully.

Brain parcellation is the process that aims to divide brain in ROIs that can be used as nodes. Before the advent of modern imaging tecniques, parcellations were based of histological analysis of the brain [53]. The idea is that different brain areas were composed by slightly different kinds of cells and cells of the same area are specialized in a determined task, so they are similar each others. Of course, this method had a lot of limitations, first of all the fact that the analysis had to be done post-mortem. Moreover, it is not trivial to extend the results for one subjects to other anatomically different brains.

With MRI and subsequent imaging methods, this process has become easier and more effective, primarily because it allowed *in vivo* analisys. The most widely used is Automated Anatomical Labeling (AAL) template, which identifies gyral and sulcal lines as boundaries of cortex and subcortical regions [54].

Harvard-Oxford (HO) Probabilistic Atlas

Another very commonly used atlas is the Harvard-Oxford (HO) probabilistic atlas [55], which identifies a number of nodes ranging from around 19 nodes of a partial network [56] to 300 nodes [57] of whole brain network. Studies that have used HO have also subparcellated the images diving each ROI into uniform sized brain areas [57, 58]. The term probalistic refers to the fact that, intead of setting precise boundaries, this parcellating method assign a voxel to each ROI with a determined probability which can be adjusting by thresholding. This is done to avoid strict boundaries assignments in order to match better ROIs with brain areas that are anatomically different in each subject. Unfortunately, this choice doesn't always leads to a perfect matching between ROIs and anatomical or functional areas [33, 59, 60], and hence, brings to node with poor correlation as discussed in 1.2.2.

HO is the atlas utilized in this work. Here, I will describe two other atlases

Spatially Constrained Spectral Clustering-Generated Atlas

Spatially Constrained Spectral Clustering-Generated Atlas is a connectivity-based parcellation method, because it is based on constructing a regular graph (lattice) before, and identify nodes by successive links removal which leads to an increased homogeneity between voxels [61]. The regular graph

is identified by assigning 26 links to each voxel (faces and edges touching). Links are weighted based on similarity between voxels. A number of clusters diving the entire volume V is set. Then an algorithm, iteratively cuts links in order to minimize a cut cost function defined as:

$$cut\,(A,B) = \sum_{v_i \in A, v_j \in B} w_{ij,} \tag{3.2}$$

where i index indicates the voxels in a cluster A and j the voxels in another cluster B, and w_{ij} is the similarity between voxels i and j, *i.e.* the link weight. Weight values are thresholded: if the distance between voxels is more than a radius ε, then $w_{ij} = 0$. Radius ε is set to include only the 26 neighbors voxels. In this way, we can identify the thresholded weight as a measure of similarity and hence, the cut cost function try to maxime similarity cutting only links between non-similar voxels. However, this minimization usually leads to cluster containing one single voxel. In order to avoid this, a Normalized Cut cost function (NCUT) [62] is defined as follow:

$$Ncut\,(A,B) = \frac{cut\,(A,B)}{\sum_{v_i \in A, v_n \in V} w_{in,}} + \frac{cut\,(A,B)}{\sum_{v \in B, v_n \in V} w_{jn,}} \tag{3.3}$$

where n index refers to all the N voxels, that are contained in the total volume V. This method has been tested with a number of clusters, *i.e.* ROIs, ranging from 50 to 1000.

Human Brainnetome Atlas

A recent approach called Human Brainnetome Atlas aims to improve some issues of other atlases, by providing a whole-brain, fine-grain and cross-validated atlas which carries information on both anatomical and functional structures [63]. As the previous method, the Human Brainnetome Atlas is said to be connectivity-based because the final procedure of parcellation follows the connectivity definition. This atlas is obtained by first dividing the raw MRI image into 34 cortical ROIs for each hemisphere and 14 subcortical ROIs. This first parcellation was done following Desikan-Killiany (DK) atlas [64].

The second step consists in applying a procedure called Probabilistic Diffusion Tractography [65]. This tecnique requires diffusion MRI (dMRI) images. DMRI is an MRI imaging tecnique which acquire a sequence of MRI

images, while a software uses the diffusion of water molecules to generate contrast in MR images [66]. In this way, thanks to dMRI, precise information about micro-structural connectivity is obtained. After the images are coregistered with the previous DK-parcellated structural images, for each voxel, the probability that a fibre pathway (or streamline) leaving a voxel will pass through other voxels is calculated. In order to do this, the probability distribution of the principal diffusion direction is estimated at each voxel. The presence of a probability distribution, instead of a single value, reflects the fact that each voxel may have different diffusion direction, plus of course the possible effects of noise and artifacts. By combining diffusion directions, it is possible to obrain a complete connectivity maps of the voxels.

In the Human Brainnetome Atlas, 5000 streamline fibers for each voxel belongin to a DK ROI are considered in order to obtain the connectivity profile of the ROI. A 2/5000 threshold is set to reduce the effect of the noise. Finally, each ROI was divived into a number of voxels clusters from 2 to 12 based on its dimension, with a clustering procedure which aimed to obtain the maximum homogeneity across ROIs. For each cluster, the probability of connection with other clusters have been computed and finally, 210 cortical ROIs and 36 subcortical ROIs have been found.

3.4 Defining Links

After nodes definition, the following step is determining the connections between nodes. There are several links definition methods for functional networks (for a comparison between methods results see [67]).

Correlation

The most intuitive and easiest method is define a link weight between a certain measure of correlation between two time series [67]. If the time series are normalized to unit variance, what we measure is normalized or full correlation. If normalization is done after excluding all of the other time series in the data (all of the nodes in the network) then what is obtained is the partial correlation. One problem with full correlation is that it could overestimate nodes connectivity [67]. If we consider a simple chain of 3 nodes, A-B-C, the presence of noise or some other external inputs could bring to assign a high value of correlation between A and C even if there is no direct connection

(sometimes, this is also how to define the difference between functional and effective networks [11]). This could bring to define the chain as a connected triangle. Using partial correlation instead, calculation of correlation between A and C is done excluding B, so no (or low) correlation will be found [67]. This method does not give any information about directionality of links.

Mutual Information

Mutual Information (MI) is a measure of the information exchanged between two variables [68]. The calculation considers both linear and non-linear dependencies, *i.e.* takes in consideration higher order statistics than correlation methods and hence, can detect connections in the network in a more sensitive way [67]. Exchanged information is obtained from individual and joint histograms comparison (for a general example of joint histograms comparison method see [69]). It is possible to calculate Partial Mutual Information considering each pair individually, *i.e.* after the other variables have been excluded. As correlation based methods, this method does not give any information about directionality of links.

Granger Causality and Related Lag-Based Measures

If we have two variables A and B, and the past of A is able to to give a better prediction of B than the past of B itself, we say that there is a causal connection between A and B. A statistical interpretation of this concept is given by Granger causality method [70]. In order to calculate a statistical measure for causality, multivariate vector autoregressive modelling (MVAR) is used. In the original paper [70], the measure indicating causality from A to B is defined as F_{AB}, and the reverse causality with F_{BA}. Other authors recomment to use $F_{AB} - F_{BA}$ in order to obtain a more robust statistical causality measure [71]. The main critique about this method is that because of the indirect nature of BOLD signal measures, Granger causality method could be influenced by systematic differences across brain regions and return several spurious values [72]. Links defined with this method are directed.

Coherence

Two signals are coherent if their phase difference is constant in a time (frequency) window. Using coherence to generate links could be useful because it

ignores delays between two registered time series (*e.g.* because of indirect nature of BOLD signal measures) [67]. Two approaches can be done, estimate coherence in a single, narrow frequency window, or in multiple frequency windows and combine later the values.

Generalized Synchronization

Synchronization is a surprising phenomenon that could be observed in many complex systems. It happens when components of the system can be modeled as oscillators, *i.e.* when the components perform a periodic motion or activity, and they are coupled with each other by certain interaction [73]. Synchronization has been observed also in the brain [19], hence it could be used to defined a link between synchronized areas. Synchrony can then evaliated "by analysing the interdependence between the signals in a state space reconstructed domain" [74]. The term generalized means that the synchronization is nonlinear.

Patel's Conditional Dependence Measures

Given two voxel time series 1 and 2, this Bayesian approach is based on calculation of $P(A_1|A_2)$, where A is a certain measure of activation [75]. Hence, $P(A_1|A_2)$ is the probability that 1 shows high activity given that 2 shows high activity after all the disturbing effects have been isolated. Given the corresponding marginal distributions $P(A_1)$ and $P(A_2)$, it is possible to define a measure κ, which define the strenght of the connection (and not yet the link weight because we are still considering voxels time series), with these properties:

- $\kappa = 0$, if 1 and 2 are statistically independent,
- κ increases with $P(A_1|A_2)$ when $P(A_1)$ and $P(A_2)$ are fixed,
- κ decreases with $P(A_1)$, as $P(A_2)$ and $P(A_1|A_2)$ are fixed, and *vice versa,* κ decreases with $P(A_2)$, as $P(A_1)$ and $P(A_1|A_2)$ are fixed.

It is also possible to define another measure $\tau \in [-1, 1]$ which identifies the directionality of the links.

Bayes Net Methods

In order to describe Bayes Net methods, I should introduce the concept of Directed Acyclic Graph (DAG). A Directed Acyclic Graph is a finite directed graph with no directed cycle, *i.e.* without nodes connected in a closed chain [76]. This kind of graphs show a particular ordering because links cannot go "backwards", but can only proceed in the direction of this ordering. A Bayesian Network or Bayesian model is basically a DAG representation where nodes are variables and links represent conditional dependencies. Bayes Net methods are based on automatic algorithms which construct networks in order to obain a Bayesian network [76, 67], where nodes (variables) are voxels time series. There are different algorithms which work in a sligthly different way (for details about each algorithm see [76]). On limited data, *i.e.* finite number of nodes, it is of course impossible to have a DAG, so the process will end at some point and the output will be the network we wanted to construct. This method is a global network modeling method because it assigns all of the links at the same time. The output is usually a directed network but with no information about the link weight. Link weight could be obtained with some modifications in the method.

LiNGAM

Linear, Non-Gaussian, Acyclic causal Models (LiNGAM) are based on an algorithm which is conceptually similar to a Bayes Net method, but instead of computing causal dependency, it utilizes higher-order statistic distributions to define network links [67]. Here, the assumption is that voxels time series (nodes) inputs follow distinct, non-Gaussian distributions, so Independent Component Analysis can be utilized. Independent Component Analysis (ICA) is a computational processing method that is used to separate a multivariate signal into its additive sub-components, assuming that there is a mutual statistical independence of the source of the non-Gaussian signals.

3.4.1 Functional Homogeneity: Spatial Consistency

As said in 1.2.2, functionally inhomogeneus ROIs are a problem in constructing a good network model for the brain because some brain areas, with different functions, can collapse into a single node without belonging effectively to that node. We also said that ROIs with poor homogeneity have components

(voxels) with poor correlation.

Poor homogenity could have two resons. First, is possible that ROI boundaries have not been set properly, so it could include voxels with different activity patterns and hence, that should belong to a different ROI. Second, it is possible that functional homogeneity varies in time [77], and this requires using dynamical network theory and tools to analyze brain networks, which is not the aim of this study.

A good measure to quantify functional homogeneity is the spatial consistency [77], defined as the mean Pearson correlation coefficient across the ROI's voxels' time series:

$$\phi(I) = \frac{1}{N_I(N_I - 1)} \sum_{i,i' \in I} C(x_i(t), x_{i'}(t)), \tag{3.4}$$

where N_I is the number of voxel inside ROI I, *i.e.* its dimension, $x_i(t)$ and $x_{i'}(t)$ are the time series of the voxels i and i', and C indicates the Pearson correlation coefficient. Sum is performed for every voxels pair belonging to ROI I. A spatial consistency value of 1 indicates perfectly homogeneous ROI, while 0 means a random collection of voxels. Although negative correlations can be found, normally $\phi \geq 0$.

3.5 Registration

3.5.1 Standard Space

The aim of registration process is to transform the data to a standard space. Data projected to a standard common space, which is the same across subjects or even studies, can be statistically analyzed and compared. Registration consists of 3 steps [37]:

1. Coregister low-resolution fMRI image in structural (anatomical) high resolution image so that they are aligned and in the same space. This can be done by identifing a transformation matrix [A], which contain the parameters needed to match the two images.

2. Normalize the structural image transforming it in order to math a template common for all the subjects. A second transformation matrix [B] is needed.

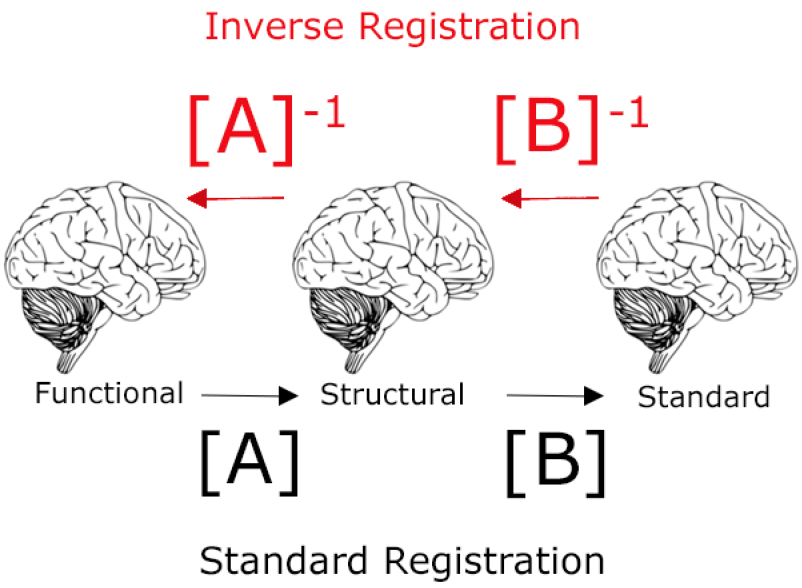

Figure 3.1: Registration in standard common space (black arrows) and inverse registration (red arrows) methods scheme. In standard registration, functional image is first coregistered with structural image using a parameters transformation matrix [A]. Then, the obtained image is transformed to a standard space, common for every subject, with the matrix [B]. In inverse registration, a template from Standard space is (inverse) registered to structural space with inverse matrix $[B]^{-1}$ and the obtained images are finally registered to the functional subject space with the matrix $[A]^{-1}$.

3. Applying the obtained parameters to the fMRI images.

The process is schematized in fig 3.1 with black arrows.

3.5.2 Inverse Registration

Although registration of images to standard space is the most commonly used normalization procedure, it presents some problems. For example, some brain areas are very different between subjects, which makes it hard to match the images into a common space. Furthermore, a universal correspondence between functional and structural images across subjects is missing. Actually, the main problem is that before co-registration, spatial smoothing should

be applied to the input image and this could lead, as said above, to some problems in output data.

In order to solve these problems, a new registration process, called inverse registration, has been developed (for a good description of the method, see [78]). The term "inverse" means that here, standard space brain areas are registered back to each subject's individual space. So, all subjects have the same number of brain areas, with same names, but the boundaries should take into account the individual anatomy of each subject.

Inverse registration is a three steps process:

1. Calculating transform matrices $[A]$ and $[B]$, but without applying them to the images.

2. Determining the inverse matrices $[A]^{-1}$ and $[B]^{-1}$.

3. Applying the matrices sequentially, from standard space to structural space with $[B]^{-1}$, and from structural space to subject functional space with $[A]^{-1}$ (fig. 3.1with red arrows).

This process basically transforms the template into the subject's native space. Furthermore, spatial smoothing is applied to the template and not in the subjects' voxels. The idea is that for these reasons, spatial consistency can be improved.

During the inverse registration process, an individual atlas should be created for every subject. In order to do this, the process of inverse registration is applied separately to every ROI. This generates a 4D image where each volume contains a ROI. The process is schematized in fig. 3.2. Because the final result will be a low resolution image, some voxels could appear to belong to different ROIs at the same time. In this case, the voxel is assigned to the ROI correspondent to its highest ROI probability value. This process is called ROI overlapping correction. If this is not sufficient and some voxels still belong to different ROIs, they should be discarded. Finally, the volumes in the 4D image are collapsed into a 3D image, which is the individual atlas, *i.e.* the map of the ROIs for that specific subject (fig. 3.3).

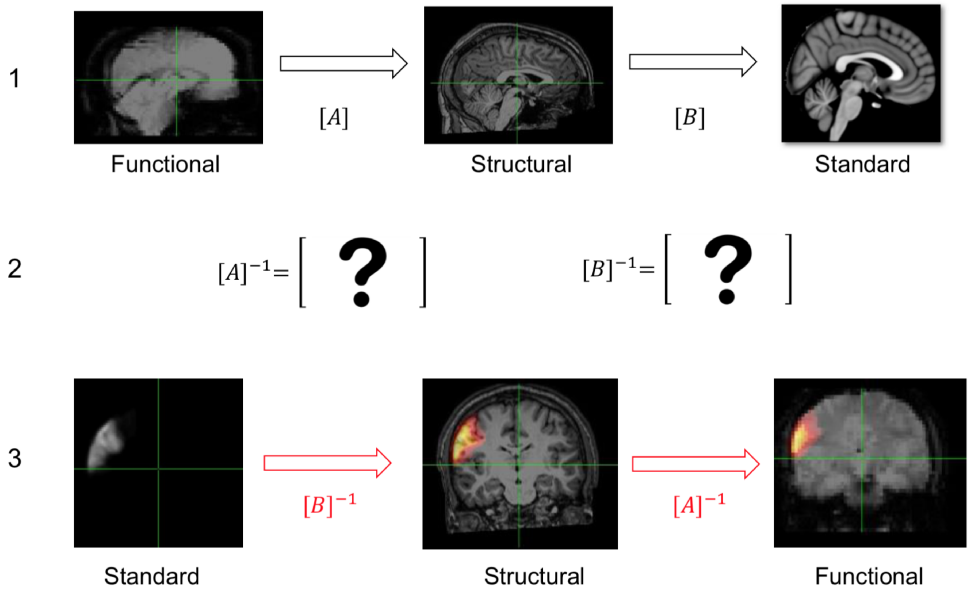

Figure 3.2: Complete inverse registration process for a single ROI. First, transformation matrices [A] and [B] are calculated. Then their inverse $[A]^{-1}$ and $[B]^{-1}$ are computed. Finally, each ROI is (inverse) registered in functional space with inverse matrix $[B]^{-1}$ and then, registered to the structural subject space with the matrix $[A]^{-1}$. In this way, each ROI takes in count the individual subject's anatomical boundaries. The process is done for every ROI and in the end, a 4-D image is obtained where each volume contains a single ROI. This image has been retrieved from [78], and reutilized with author's permission.

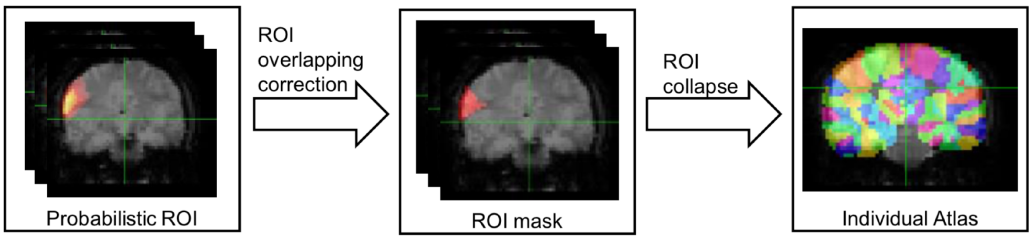

Figure 3.3: Merging of 4D output image of an inverse registration complete process. In the first step of ROI overlapping correction, voxels that belong to more than one ROI are assigned to the ROI with maximum probability. If this doesn't solve the problem, voxels are discarded. ROIs are then masked. The second step is collapsing the volumes of the 4D image into a 3D image which represent the individual atlas. This image has been retrieved from [78], and reutilized with author's permission.

Part II

Practical Applications

Chapter 4

Materials and Methods

The results of this thesis has been obtained on data used before in another work [78], for which it was selected, checked and preprocessed. In this chapter, a resume of those processes of data selection is presented, together with tools and methods.

4.1 ABIDE Database

ABIDE (Autism Brain Imaging Data Exchange) is the most used open database of brain fMRI data from subjects with autism spectrum disorder (ASD), simply known as autism [79].

ABIDE database was released in June 2014 and since then, new data has been added. ABIDE I is the first release and contains samples for 539 subjects with ASD and 573 control subjects (healthy), from 17 different international institutes [79]. ABIDE II is the second release and updated the first with 487 ASD samples and 557 controls subjects, from 19 sites [80]. In ABIDE it is also possible to find preprocessed data by different preprocessing tools and methods [81]. Data is matched with phenotypic information about the subjects and it is completely anonymous and without protected health information.

4.1.1 Subject Selection

Subject selection has been done in another work [78], here I will include a brief resume. For the aims of this study, raw NIFTI files have been used

Dataset	Release	Effective ASD/TC Number	ASD age range	TC age range
ETH Zurich	II	11/22	18.5-24.5	18-30
Trinity Centre for Health Sciences	II	6/7	18.5-19.5	19-20
University of Utah School of Medicine	II	3/9	22-38.5	18.5-36
NYU Langone Medical Center	I	14/23	19.5-39	18.5-31
University of Utah School of Medicine	I	35/28	18-50	18-39

Figure 4.1: Included datasets from ABIDE, after sex and age filtering criteria, selected to obtain the maximum number of subjects and, contemporarily, the best dataset homogeneity. Name of the dataset, ABIDE release, number of ASD and TC subject (after FIQ control), and age range are shown. University of Utah School of Medicine data from both releases are present, in order to improve homogeneity in the sample. This table has been retrieved from [78], and reutilized with author's permission.

in order to preprocess using inverse registration (see 3.5 for a description of the method). The next step was choosing data to have as many subjects as possible. In order to do this, male subjects have been choosed because autism incidence is higher in male than in female [82], and older than 18 because brain in young people is still evolving and changing [83]. Following those criteria, 5 databases have been selected (fig. 4.1). From these datasets, only individual with full intelligence quozient within 2σ standard deviation (108 ± 15) were selected. After that, an image quality control was done for the 158 subjects selected after preliminar filtering. In total, three controls have been done: to raw structural and fMRI data, to preprocessed structural MRI and in the end, to functional data. Functional data quality control in particular has been done to check if inverse registration was succesfull, *i.e.* good matching between ROIs and brain image, or not. An example of good and bad results of inverse registration are shown in fig. 4.2.

Only 66 subjects passed quality control check. Half of that, were TC and in order to avoid possible modification in brain structure due to ASD, I

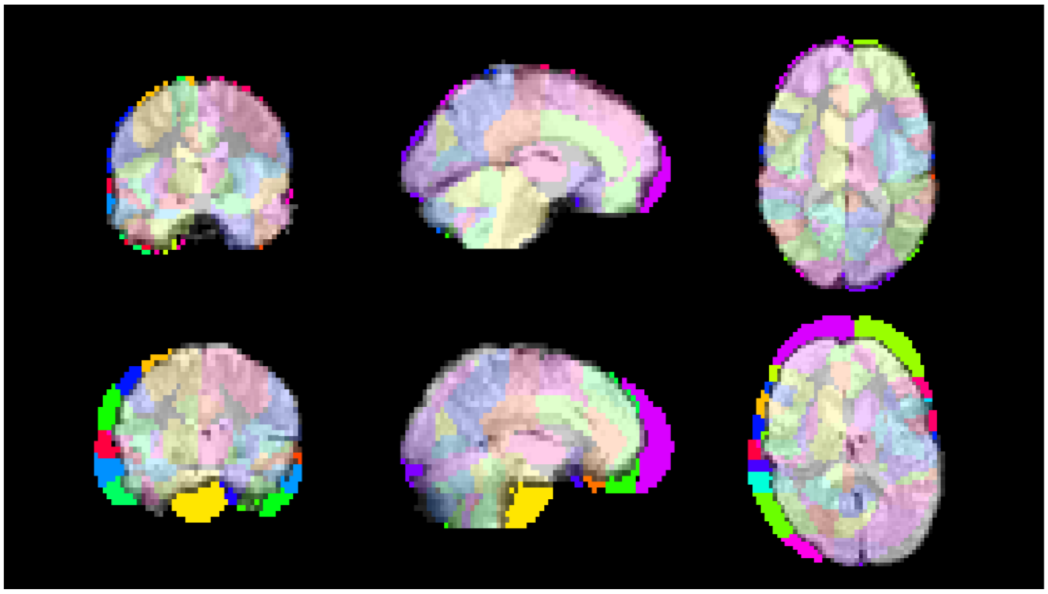

Figure 4.2: Example of succesfull atlas inverse registration (top row) and unsuccessfull atlas inverse registration (bottom row). It is possible to note how in successfull inverse registration almost all ROIs match the brain image, while in unsuccesfull inverse registration most of the ROIs are not matching the brain image. This image has been retrieved from [78], and reutilized with author's permission.

only selected the 33 healthy control subjects to perform all of the analises. Preprocessing has been performed with FSL software: non-brain tissue was removed and head motion corrected (for all the details see [78]). Spatial smoothing has not been applied.

4.2 Network Construction and Analysis

4.2.1 Node Definition

Data was processed using the HarvardOxford parcellation thresholded at 30% of probability, whereas in the inverse-registration process, the parcellation was not thresholded. Instead, the strongest probability for each ROI has been kept. Since this is a standard procedure, a group mask, *i.e.* maps that tell which voxels belong to which ROI, was created and based on that mask, the ROI maps were computed. During this procedure, one ROI was lost, *i.e.* it was not present in any of the inverse-registered subjects. This means that networks with inverse-registered nodes posses one node less than standard space brain networks. In any case, this is assumed not to bea problem for network analysis.

4.2.2 Link Definition

In order to properly define links, we first identify a ROI time series as the unweighted average of the time series of its voxels:

$$X_I(t) = \frac{1}{N_I} \sum_{i \in I} x_i(t), \tag{4.1}$$

where N_I is the number of voxels inside ROI I, *i.e.* its size, and $x_i(t)$ is the time series of voxel i. Then, link weights between two ROIs are calculated as the pearson coefficients between ROIs time series [39]. This is a typical procedure that lead to all-to-all connected weighted undirected networks.

For some of the network measures, I thresholded the network, in order to keep only 10% percent of the strongest link and discard the rest, obtaining a unweighted networks. Furthermore, this procedure yielded to negative correlations, and hence negative link weights, which some authors recommends to discard [93], but they have been kept in order to obtain smoother distributions of some of the network measures (see 5.2.3 and 5.6).

4.2.3 Network Analysis

In order to compare network measures between networks with inverse registered nodes and networks with standard space nodes, what is calculated is the Probability Density Distributions (PDF) *i.e.* the probability that a random variable falls within a particular range of values. In a rigorous way, PDF should be defined for a continuous variable (even if there are ways to define it for non-continuous variable), but some parameters, like degree or path lenghts, are discrete values so the functions will look more like a normalized probability histogram. Since we are mainly interested in a qualitative comparison this does not significantly affect the results.

Network adjacency matrices and voxel's time series has been saved in Matlab ".mat" files and loaded with Python programming language. Network analysis was performed with NetworkX Python library, which define networks as a dictionary where keys are node pairs and values represent the link weight between those nodes. The Python code containing the functions for calculating spatial consistency was retrieved from another study [84]. I only created a new frontend script and defined parameters in order to adapt the code to the data used on this study.

Chapter 5

Results

In this chapter, I will present the results of this study. Firs of all, I will present spatial consistency probability density plot for both networks with ROIs registered in standard space, and for the networks with inverse-registered ROIs in order to inspect the differences and see if the hypothesis of increased functional homogeneity of inverse-registered ROIs is valid. Then, I will show the principal network measures described in detail in chapt. 2, again in comparison between the two kind of networks, in order to spot and discuss eventual differences. A similar comparison for degree, clustering coefficient, path lenght and assortativity distributions has been made in another study [85], so I will also discuss if the results are consistent.

5.1 Spatial Consistency

The plot of the distributions of spatial consistency probability density across all the ROIs is shown in figure 5.1. It is evident that inverse registration leads to increased spatial consistency while standard space ROIs are internally less homogeneous. As discussed in 3.4.1, ROIs with 0 consistency are a random collection of non-correlated voxels; we can see that standard space ROIs spatial consistency distribution is really close to that value. Even without considering the consistency distribution of inverse registered ROIs, this result already suggests that standard-space ROIs are not a good way to define nodes. The price for having a common space to make different subjects comparable is too high and hence new methods are strongly recommended. Of course, the inverse-registered ROIs don't yet have values very close to

one, which whould mean an almost perfect correlation. However, the inverse registration approach surely is already a huge improvement.

5.2 Network Properties Comparison

Now that we prove that inverse registration leads to ROIs with a higher spatial consistency than the ones defined in standard space, we are interested in network measures to see if there are changes between the two kind of networks. The properties whose distributions we want to compare are described in details in chapter 2.

5.2.1 Degree Distribution

The plot of the distributions of node degree is shown in figure 5.2 in a lin-lin plot, and in figure 5.3 in a log-log plot. Thresholded networks have been used keeping only the strongest 10% of the links. In order to obtain a relatively smooth line, degree values are divided into 11 bins.

As we can see, the two distributions are very similar. Networks with inverse registered nodes seem to have slightly more higher degree nodes ($L > 35$) in comparison to standard space networks. This slight difference across degrees is consistent with the results of another similar study [85].

The shape of the distribution in log-log plot is consistent with the one obtained in another study which did not use inverse registration; in such study, data was fitted well with power-law distribution with exponential cut-off [86] which is a distribution found on a lot of different kind of networks, for example WWW [87], protein networks [88], scientific collaboration networks [89], etc.

5.2.2 Clustering Coefficient Distribution

The plot of the distributions of node clustering is shown in figure 5.4. Also here, networks thresholded to 10% of the strongest links have been used because, as discussed in section 2.2.2, we focused on unweighted clustering coefficient.

The two distributions are basically the same. Of course there are several nodes with clustering 0 because in scale-free networks we expect nodes with degree 0 and 1to be high in number, and for those nodes, clustering value is 0

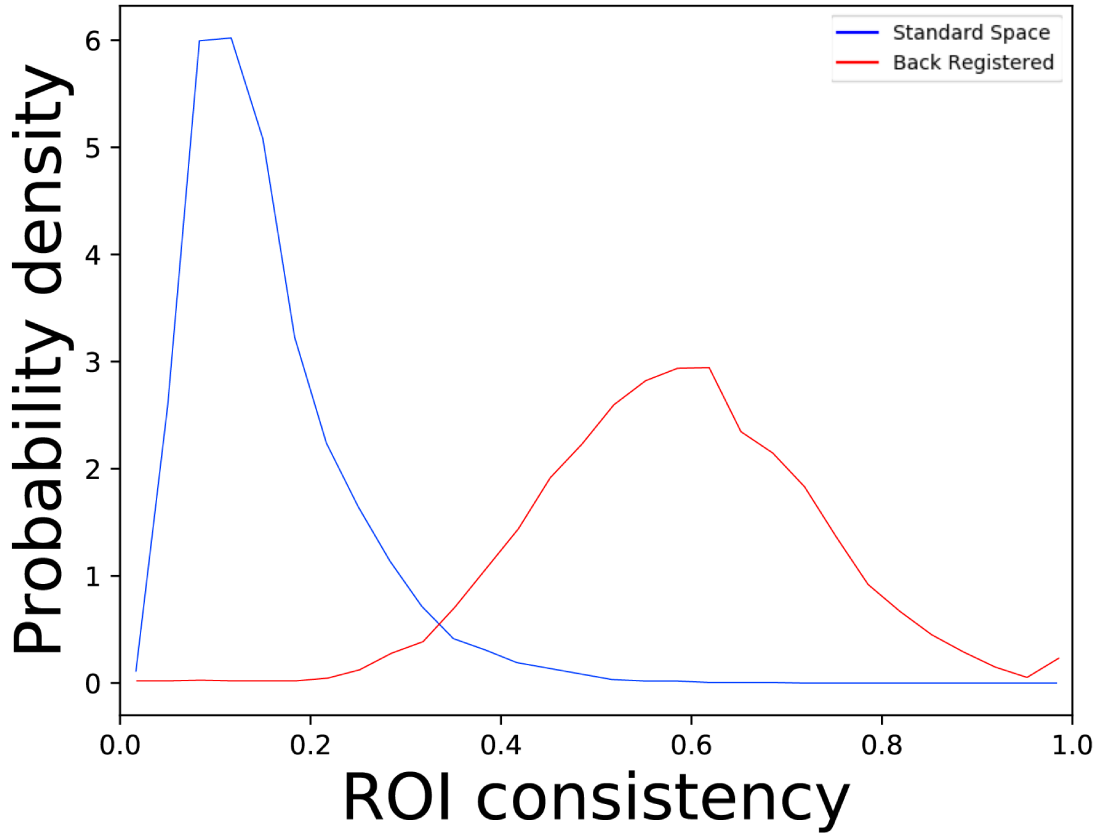

Figure 5.1: Probability density function of spatial consistency for networks with nodes defined in standard space (in blue) and with inverse registered nodes (in red), calculated over all ROIs. Registration into standard space leads to ROIs with homogeneity close to 0, suggesting that this is not a good method to define nodes. Inverse registration leads to much higher spatial consistency and thus better nodes, although it is still not very close to the value 1.

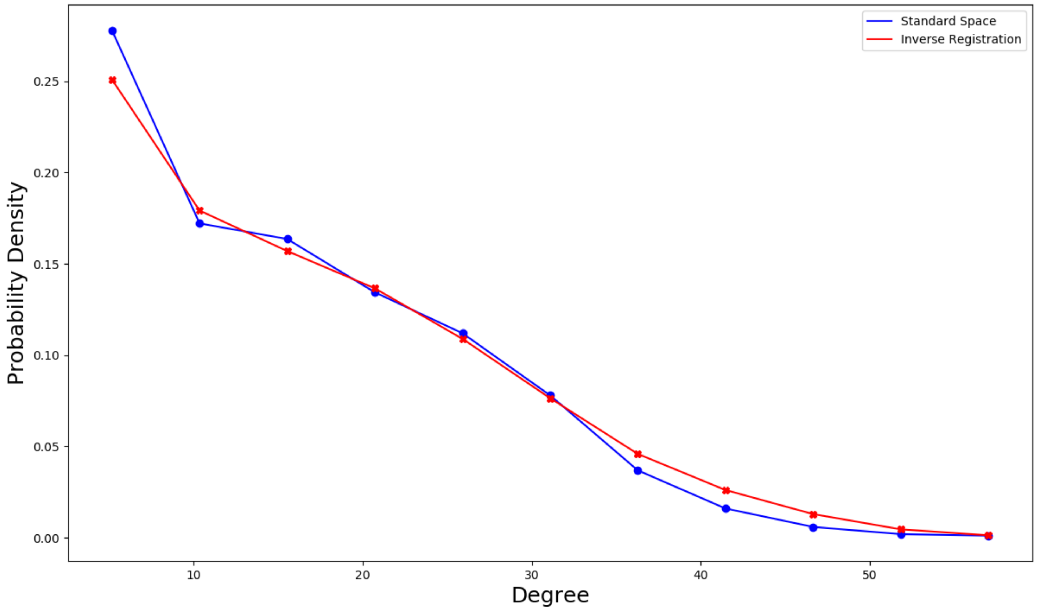

Figure 5.2: Degree probability density function for networks with nodes defined in standard space networks (in blue) and with inverse registered nodes (in red) over degree values. Degree values are divided into 11 bins. Data has been collected from 10% thresholded networks. The number of inverse-registered higher degree nodes seem to be quite higher respect of standard-registered nodes. Both distributions are scale-free but rnot exactly power-law distributions (as can be better observed in fig. 5.3).

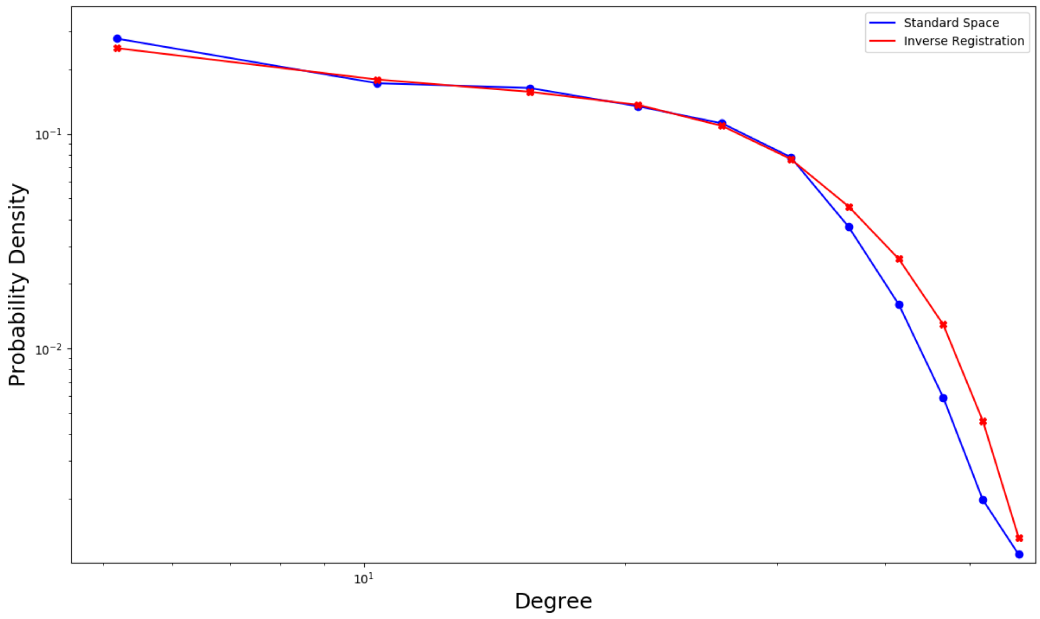

Figure 5.3: Degree probability density function for for networks with nodes defined in standard space networks (in blue) and with inverse registered nodes (in red) over degree values in a log-log plot. Degree values are divided into 11 bins. Data has been collected from thresholded networks keeping only 10% of the strongest links. It is clearly evident that the distributions are not perfect power-law, but it may be a power law with exponential cutoff which was found in other brain networks and other kind of networks (see 5.2.1 for details).

by definition. Clustering coefficient values lay mainly in the region between 0.4 and 0.6 and higher values are more present than lower ones. Average clustering for both kind of networks are all very close to 0.47. These values are consistent with a similar study [85], and it may be a good indicator of the small-world property as found from other authors [90], although small-worldness of brain networks is still controversial [91]. Indeed, it was observed that small-worldness property may be observed because of inaccuracies in data and consequent preprocessing methods [91]. Furthermore, even if the brain is really a small-world network, is still challenging to find a statisfactory functional meaning [91].

The plot of the $C(k)$ function 2.8is shown in figure 5.5. It is interesting to note that values of inverse registered nodes appear to fluctuate less, especially in extremely low degree and high degree regions. Values of $C(k)$ tend to decrease with k, *i.e.* smaller nodes have a higher local clustering coefficient than hubs. Hence small degree nodes have a more dense neighborhoods than hubs. This is a consequence of hierarchy [92]: we can say that small degree nodes belong to small dense communities, while hubs tend to create "bridges" between different communities by linking them. A similar behavior has been observed in WWW, scientific collaboration networks, metabolic and protein networks [92]. This could suggest that brain areas work together in order to attempt specific tasks.

5.2.3 Link Weight Distribution

The distributions of link weight are shown in figure 5.6. In this case, non-thresholded networks have been used for both networks with nodes defined in standard space and with inverse registered nodes. We can see that the shape of the distributions is very similar. However, link weight distribution of networks with inverse registered nodes is a little bit shifted towards higher values. This is not surprising: with increased spatial consistency (ROIs functional homogeneity) we expected stronger links. Negative values can be interpreted as negative action of the links (inhibition) but a clear interpretation is still missing. They should be removed before the analysis of the network until when, possibly, future network methods will be able to clarify the role of negative weights [93].

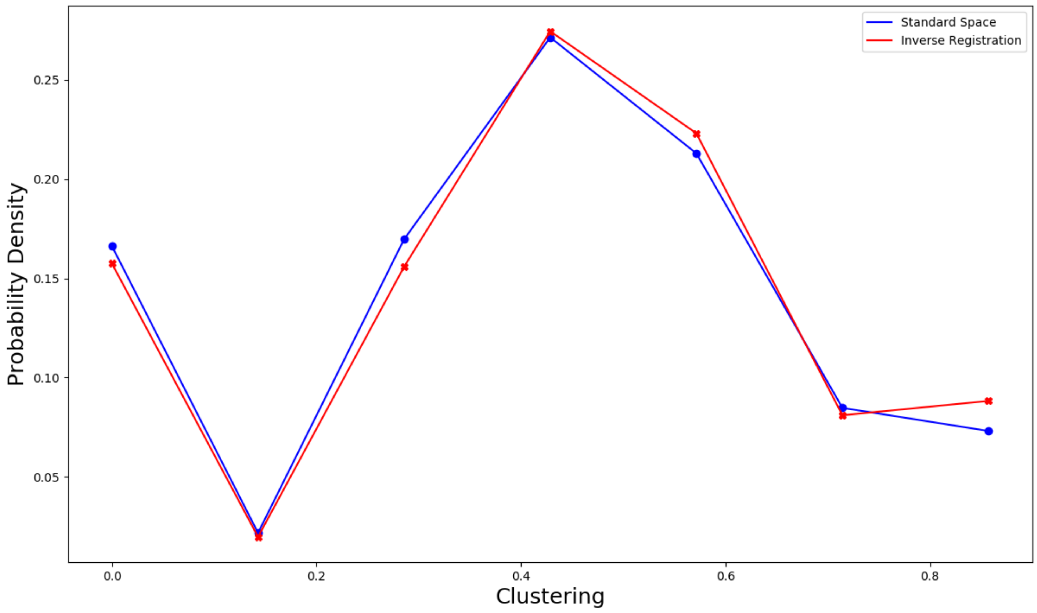

Figure 5.4: Probability density function of unweighted clustering for networks with nodes defined in standard space (in blue) and with inverse registered nodes (in red). Clustering values are divided into 10 bins. There are no big differences between the distributions. Average clustering is quite high compared to random networks, and this could be a good indicator of the small-world property.

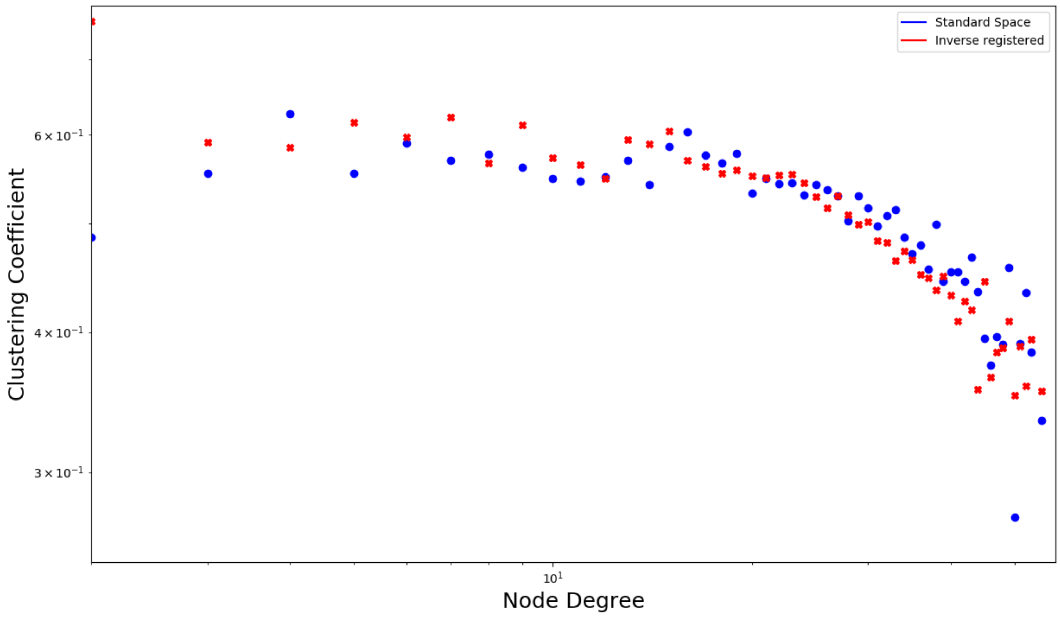

Figure 5.5: Average clustering coefficient over nodes with same degree in function of node degree for networks with nodes defined in standard space (in blue) and with inverse registered nodes (in red). Clustering values of inverse registered nodes fluctuates less, in extremely low degree and high degree regions. The fact that $C(k)$ decreases with k could be a consequence of the organization of the brain networks in communities.

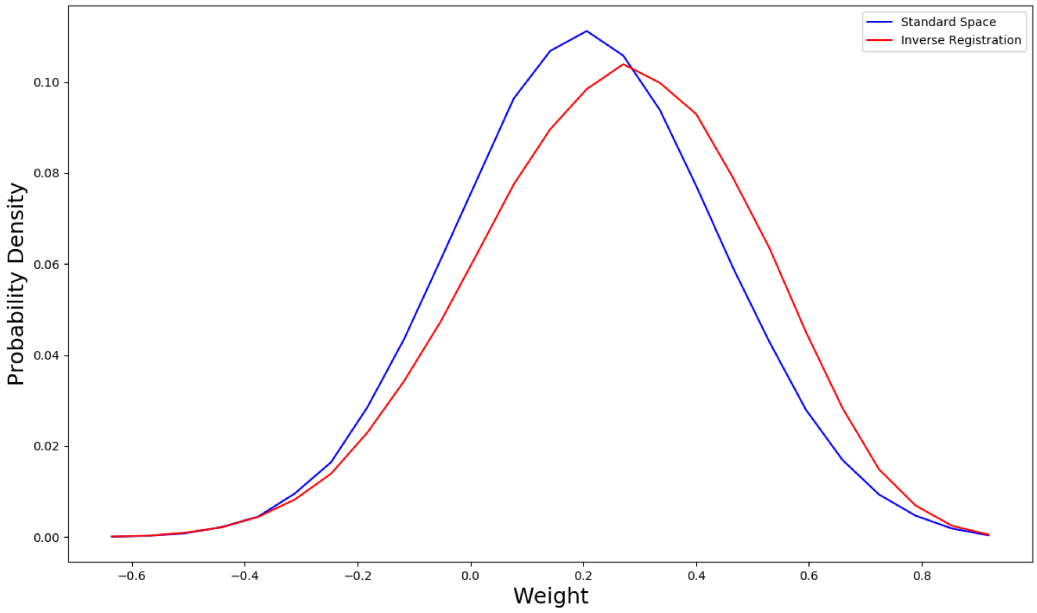

Figure 5.6: Link weight probability density function for networks with nodes defined in standard space (in blue) and with inverse registered nodes (in red). Weight values are divided into 25 bins. Nonthresholded networks have been used. Distribution for networks with inverse registered nodes is a little bit shifted towards higher values, probably because the increased functional homogeneity between ROIs. Negative values are typically present but a clear interpretation is still missing.

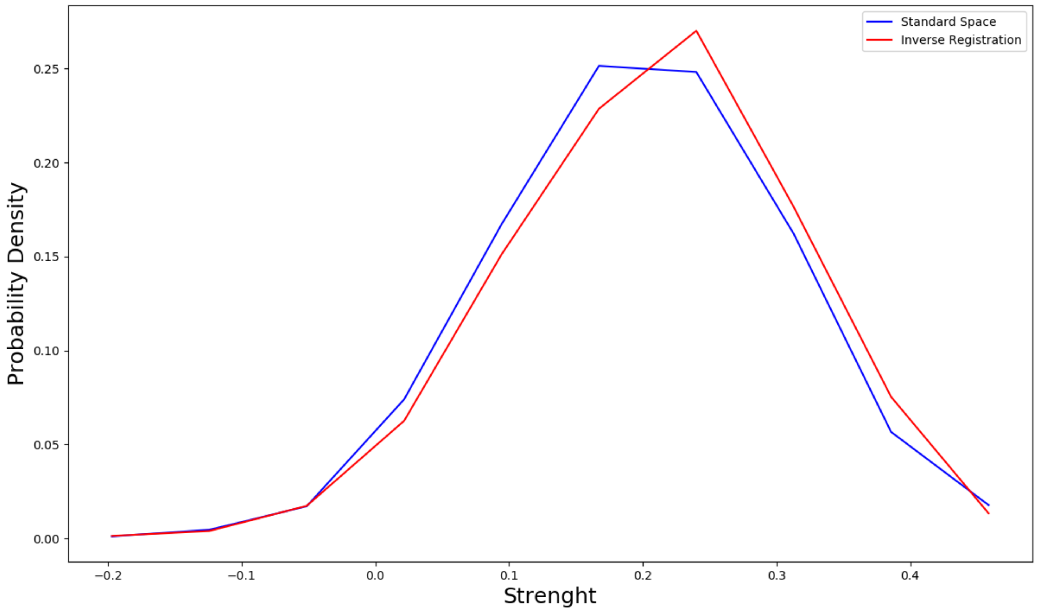

Figure 5.7: Probability density function of strenght for networks with nodes defined in standard space (in blue) and with inverse registered nodes (in red). Strenght values are divided into 13 bins. Nonthresholded networks have been used. Similarly as for link weight, distribution for inverse registered nodes is shifted towards higher strenght values.

5.2.4 Strenght Distribution

The plot of the distributions of node strenght is shown in figure 5.7. Nonthresholded networks have been used. As expected following the weight distribution, we can observe a shift towards higher values of strenght for inverse registered nodes and the presence of negative values.

5.2.5 Path Lenght (Distance) Distribution

The distributions of path lenght are shown in figure 5.8. Thresholded networks have been used keeping only the strongest 10% of the links. The distributions are basically the same.

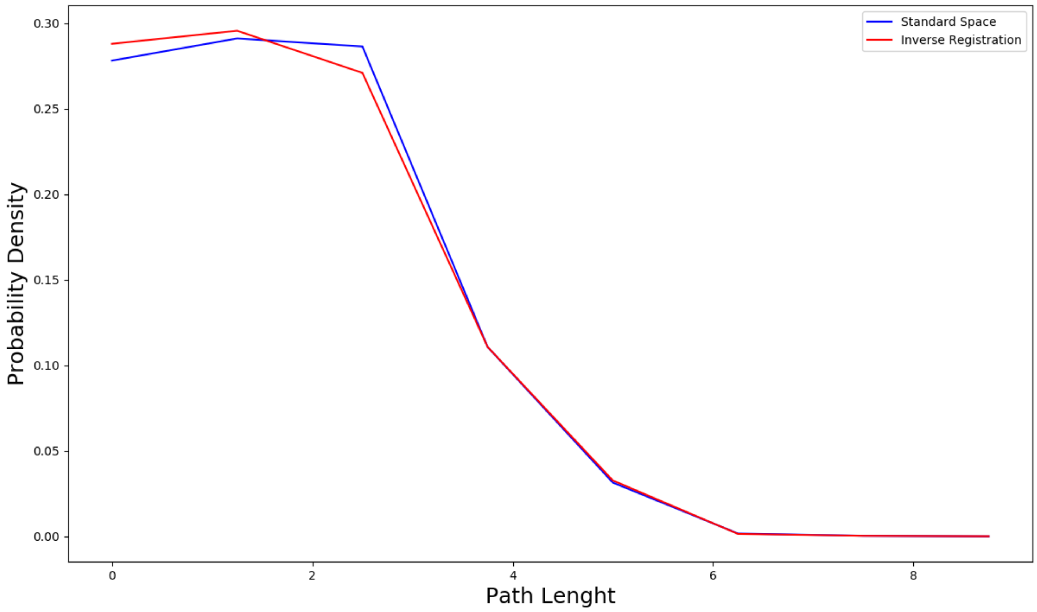

Figure 5.8: Probability density function of shortest path lenght for networks with nodes defined in standard space (in blue) and with inverse registered nodes (in red). Path lenght values are divided into 8 bins. Thresholded networks with 10% of the strongest links have been used. Distributions are very similar.

The average shortest path lenghts was 2.06 for standard-space networks and 1.98 for networks with inverse registered nodes, slightly higher than the result obtained in a similar study [85].

5.2.6 Assortativity

The assortativity distributions are shown in figure 5.9. Thresholded networks with 10% of the strongest links have been used. It is difficult to draw conclusions about the shape of the distributions. Assortativity values are positive and close to the ones found before in a similar study [85].

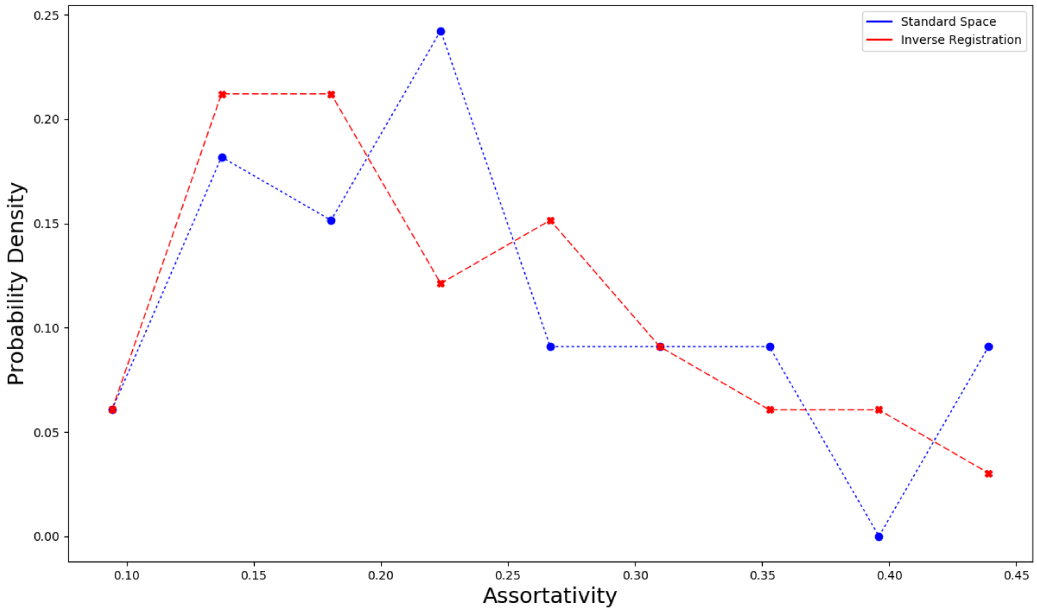

Figure 5.9: Probability density function of assortativity for networks with nodes defined in standard space (in blue) and with inverse registered nodes (in red). Assortativity values are divided into 8 bins. Thresholded networks with 10% of the strongest links have been used. Irregular distributions and results similar to other study [85].

Chapter 6

Conclusions

Modeling brain as a network in order to use the power of the tools of network science gives us new extraordinary insights about one of the most complex systems in the known universe. However, a universal accepted method for defining nodes in functional brain networks is still missing. In this thesis, I validated the use of inverse-registration method and the results are really encouraging. In inverse registration the templates from standard space are (inverse) registered to structural space and the obtained images are registered to the functional subject space. The spatial consistency, *i.e.* a measure of functional homogeneity of ROIs (how similar they are), had a huge improvement for inverse-registered nodes than nodes registered in standard space. Although this should be a sufficient reason to prefer this new method, it is still interesting to outline the fact that nodes registered in a standard space have a very low spatial consistency. Moreover, the comparison between network properties has shown some significant differences. Degree, link weight, strenght and assortativity distributions had shown slight differences, while clustering and path lenght distributions were basically the same. However, the results are mostly still consistent with another study that I used as reference [85] and with general theoretical results.

These results can suggest that standard space registration method should be discarded *a priori*. However, since inverse registration is a very recent method, this work is actually, to the best of my knowledge, the first validation of it using spatial consistency. Another study had the goal to validate inverse registration , and the results for network analysis were consistent to the ones in this work.

This thesis was based on data with a specific parcellation method with a

specific threshold and a specific way to defining links, among several others. Also the dataset (33 subjects) is relatively small. For all of these reasons it is still soon to generalize the results. There are still many possibilities to further validate the new method, for example usind different raw data, like from electroencephalography (EEG) or magnetoencephalography (MEG), using different parcellation or link defining methods. Validating inverse registration in different environments will also be useful to spot differences in functional homogeneity variations, for example if there are combinations of methods which can lead to a even higher functional homogeneity than the one found in this work. Other studies were done using inverse registration approach, but they don't contain any validation of it [93, 94, 95].

A general validation of inverse registration could open to even more research to see if new insights about brain network properties will be found. Of course, since this research line is relatively young, we should be keen to eventually modify, adapt or completely drop some of the tools that have been used until today. What said is also applicable to inverse registration, since even a more general validation should take into account that the results are not perfect and probably a new method could define nodes with an even higher functional homogeneity.

Anyway, the results of this work are a good starting point, both to open new insights on functional brain networks and to be a step to bring us closer to a universal method to define nodes. This should be a research line parallel to the improvement of data acquiring and processing tecniques in order to give Network Neuroscience, a relatively young discipline, more powerful tools to face the hard challenges of the next years.

Bibliography

[1] Bar-Yam, Yaneer (2002). "General Features of Complex Systems" (PDF). Encyclopedia of Life Support Systems. EOLSS UNESCO Publishers, Oxford, UK. Retrieved 16 September 2014.

[2] A. L. Barab´asi, R. Albert (2002). "Statistical mechanics of complex networks". Reviews of Modern Physics. 74: 47–94. arXiv:cond-mat/0106096 Freely accessible. Bibcode:2002RvMP...74...47A. doi:10.1103/RevModPhys.74.47.

[3] M. E. J. Newmann. (2003). The structure and function of complex networks. SIAM Review. 45(2): 167-256.

[4] Williams RW, Herrup K (1988). The control of neuron number. Annual Review of Neuroscience. 11 (1): 423–53.

[5] Drachman D (2005). Do we have brain to spare?. *Neurology. 64 (12)*: 2004–5.

[6] Faure, P., Korn, H. (2001). Is there chaos in the brain? I. Concepts of nonlinear dynamics and methods of investigation. *Comptes Rendus de l'Académie des Sciences - Series III - Sciences de la Vie, 324(9),* 773-793.

[7] Rubinov, M., Sporns, O., Thivierge, J. F., Breakspear, M. (2011). Neurobiologically Realistic Determinants of Self-Organized Criticality in Networks of Spiking Neurons. *PLOS Computational Biology,* e1002038

[8] Towlson, E. K., Vértes, P. E., Ahnert, S. E., Schafer, W. R., and Bullmore, E. T. (2013). The rich club of the C. elegans neuronal connectome. J. Neurosci. 33, 6380–6387. doi: 10.1523/JNEUROSCI.3784-12.2013

[9] Sporns, O. (2013b). Network attributes for segregation and integration in the human brain. Current Opinion in Neurobiology, 23(2), 162–171. doi:10.1016/j.conb.2012.11.015

[10] Tononi, G., Sporns, O., & Edelman, G. M. (1994). A measure for brain complexity: Relating functional segregation and integration in the nervous system. Proceedings of the National Academy of Sciences of the United States of America, 91(11), 5033–5037.

[11] Friston, K. J. (1994). Functional and effective connectivity in neuroimaging: A synthesis. Human Brain Mapping, 2(1-2), 56–78.

[12] Wang, J., Wang, L., Zang, Y., Yang, H., Tang, H., Gong, Q., et al. (2009). Parcellation-dependent small-world brain functional networks: a resting-state fMRI study. Hum. Brain Mapp. 30, 1511–1523. doi: 10.1002/hbm.20623

[13] Eguíluz, V. M., Chialvo, D. R., Cecchi, G. A., Baliki, M., and Apkarian, A. V. (2005). Scale-free brain functional networks. Phys. Rev. Lett. 94:018102. doi: 10.1103/PhysRevLett.94.018102

[14] Butts, C. T. (2009). Revisiting the foundations of network analysis. Science 325, 414–416. doi: 10.1126/science.1171022

[15] Schmahmann, J.D., Pandya, D.N., 2007. Cerebral white matter — historical evolution of facts and notions concerning the organization of the fiber pathways of the brain. J. Hist. Neurosci. 16, 237–267.

[16] Caspers, S., Eickhoff, S. B., Zilles, K., & Amunts, K. (2013). Microstructural grey matter parcellation and its relevance for connectome analyses. NeuroImage,80,18–26. doi:10.1016/j.neuroimage.2013.04.003

[17] Sporns, O. (2013). The human connectome: Origins and challenges. NeuroImage. 80, 53-61.

[18] Traub, R.D., Miles, R., Wong, R.K., 1989. Model of the origin of rhythmic population oscillations in the hippocampal slice. Science 243, 1319–1325.

[19] Sporns, O., Gally, J.A., Reeke, G.N., Edelman, G.M., 1989. Reentrant signaling among simulated neuronal groups leads to coherency in their oscillatory activity. Proc. Natl. Acad. Sci. U. S. A. 86, 7265–7269.

[20] Le Bihan, D., Johansen-Berg, H., 2011. Diffusion MRI at 25: exploring brain tissue structure and function. NeuroImage 61, 324–341.

[21] Sejnowski TJ, Churchland PS, Movshon. JA. (2014). Putting big data to good use in neuroscience. Nat Neurosci. 17(11), 1440-1.

[22] Bassett, D. S., & Sporns, O. (2017). Network neuroscience. Nature Neuroscience, 20(3),353. doi:10.1038/nn.4502

[23] Hasson, U., Nir, Y., Levy, I., Fuhrmann, G., & Malach, R. (2004). Intersubject synchronization of cortical activity during natural vision. Science, 303(5664),1634–1640. doi:10.1126/science.1089506

[24] Sporns, O., Tononi, G., & Kötter, R. (2005). The human connectome: A structural description of the human brain. PLoS Computational Biology, 1(4), e42. doi:10.1371/journal.pcbi.0010042

[25] Stam, C. J. (2004). Functional connectivity patterns of human magnetoencephalographic recordings: A 'small-world' network? NeuroscienceLetters,355(1),25–28. doi:10.1016/j.neulet.2003.10.063

[26] Muldoon, S. F., & Bassett, D. S. (2016). Network and multilayer network approaches to understanding human brain dynamics. Philosophy of Science,83(5),710–720. doi:10.1086/687857

[27] Palva, S., & Palva, J. M. (2012). Discovering oscillatory interaction networks with M/EEG: Challenges and breakthroughs. Trends in Cognitive Sciences, 16(4),219–230. doi:10.1016/j.tics.2012.02.004

[28] Rubinov, M., Sporns, O. (2010). Complex network measures of brain connectivity: Uses and interpretations. *NeuroImage, 52(3),* 1059-1069.

[29] Betzel, R. F., & Bassett, D. S. (2016). Multi-scale brain networks. NeuroImage. (Advanceonlinepublication.) doi:10.1016/j.neuroimage.2016.11.006

[30] Bassett, D. S., & Bullmore, E. T. (2009). Human brain networks in health and disease. Current Opinion in Neurology, 22(1653), 340–347. doi:10.1097/WCO.0b013e32832d93dd

[31] Papo, D., Zanin, M., Pineda-Pardo, J. A., Boccaletti, S., & Buldú, J. M. (2014). Functional brain networks: Great expectations, hard times and the big leap forward. Philosophical Transactions of the Royal Society B, 369(1653), 20130525. doi:10.1098/rstb.2013.0525

[32] Smith, S. M., Miller, K. L., Salimi-Khorshidi, G., Webster, M., Beckmann, C. F., Nichols, T. E., et al. (2011). Network modelling methods for FMRI. Neuroimage 54, 875–891. doi: 10.1016/j.neuroimage.2010.08.063

[33] Stanley M.L., Moussa M.N., Paolini B.M., Lyday R.G., Burdette J.H. and Laurienti P.J. (2013) Defining nodes in complex brain networks. *Front. Comput. Neurosci. 7:169.* doi: 10.3389/fncom.2013.00169

[34] Liu, J., Qin, W., Yuan, K., Li, J., Wang, W., Li, Q., et al. (2011). Interaction between dysfunctional connectivity at rest and heroin cues-induced brain responses in male abstinent heroin-dependent individuals. PLoS ONE 6:e23098. doi: 10.1371/journal.pone.0023098

[35] Power, J. D., Cohen, A. L., Nelson, S. M., Wig, G. S., Barnes, K. A., Church, J. A., et al. (2011). Functional network organization of the human brain. Neuron 72, 665–678. doi: 10.1016/j.neuron.2011.09.006

[36] Stevens, A. A., Tappon, S. C., Garg, A., and Fair, D. A. (2012). Functional brain network modularity captures inter- and intra-individual variation in working memory capacity. PLoS ONE 7:e30468. doi: 10.1371/journal.pone.0030468

[37] M, Holden A review of geometric transformations for nonrigid body registration. IEEE Trans Med Imaging, 27 (2008) , p 111-128

[38] Hayasaka, S., and Laurienti, P. J. (2010). Comparison of characteristics between region-and voxel-based network analyses in resting-state fMRI data. Neuroimage 50, 499–508. doi: 10.1016/j.neuroimage.2009.12.051

[39] Alakörkkö, T., Saarimäki, H., Glerean, E., Saramäki, J., Korhonen, O. (2017). Effects of spatial smoothing on functional brain networks. *European Journal of Neuroscience, 46,* 2471-2480. doi:10.1111/ejn.13717.

[40] Craddock, R. C., James, G. A., Holtzheimer, P. E., Hu, X. P., and Mayberg, H. S. (2012). A whole brain fMRI atlas generated via spatially

constrained spectral clustering. Hum. Brain Mapp. 33, 1914–1928. doi: 10.1002/hbm.21333

[41] Barabási, A.-L. (2016). Network Science. Cambridge University Press.

[42] D. J. Watts and S. H. Strogatz. (1998). Collective dynamics of 'small-world' networks. Nature, 393: 409–10.

[43] A. Barrat, M. Barthélemy, R. Pastor-Satorras, A. Vespignani. (2004) The architecture of complex weighted networks. Proceedings of the National Academy of Sciences, 101 (11) 3747-3752; DOI: 10.1073/pnas.0400087101

[44] M. E. J. Newman. Assortative mixing in networks. Phys. Rev. Lett., 89: 208701, 2002.

[45] Barabási, A.-L., Albert, R. (1999). Emergence of scaling in random networks. Science, 286 (5439).

[46] Hanson, L. G. (2008). Is quantum mechanics necessary for understanding magnetic resonance? Concepts in Magnetic Resonance Part A, 32(5), 329– 340. doi:10.1002/cmr.a.20123

[47] Logothetis, N. K. (2008). What we can do and what we cannot do with fMRI. Nature,453(7197),869–878. doi:10.1038/nature06976.

[48] Bandettini, P. A., Wong, E. C., Hinks, R. S., Tikofsky, R. S., & Hyde, J. S. (1992). Time course EPI of human brain function during task activation. Magnetic ResonanceinMedicine,25(2),390–397. doi:10.1002/mrm.1910250220

[49] Attwell, D., Buchan, A. M., Charpak, S., Lauritzen, M., MacVicar, B. A., & Newman, E. A. (2010). Glial and neuronal control of brain blood flow. Nature, 468(7321), 232–243. doi:10.1038/nature09613

[50] Uğurbil, K., Adriany, G., Andersen, P., Chen, W., Gruetter, R., Hu, X., ... Ogawa, S. (2000). Magnetic resonance studies of brain function and neurochemistry. Annual review of Biomedical Engineering, 2(1), 633–660. doi:10.1146/annurev.bioeng.2.1.633

[51] K.J. Friston, O. Josephs, E. Zarahn, A.P. Holmes, S. Rouquette, J.-B. Poline, To Smooth or Not to Smooth?: Bias and Efficiency in fMRI Time-Series Analysis, NeuroImage, Volume 12, Issue 2, August 2000, Pages 196-208, ISSN 1053-8119, http://dx.doi.org/10.1006/nimg.2000.0609.

[52] JV. Hajnal, R. Myers, A. Oatridge, JE. Schwieso, IR. Young, GM. Bydder Artifacts due to stimulus-correlated motion in functional imaging of the brain. Magn Reson Med, 3 (1994), p283–291.

[53] Brodmann, K. (1909). Vergleichende Lokalisationslehre der Grosshirnrinde in ihren Prinzipien dargestellt auf Grund des Zellenbaues. Leipzig: Verlag von Johann Ambrosius Barth.

[54] Tzourio-Mazoyer, N., Landeau, B., Papathanassiou, D., Crivello, F., Etard, O., Delcroix, N., . . . Joliot, M. (2002). Automated anatomical labeling of activations in SPM using a macroscopic anatomical parcellation of the MNI MRI single-subject brain. NeuroImage, 15(1), 273–289. doi:10.1006/nimg.2001.0978

[55] Desikan, R. S., Ségonne, F., Fischl, B., Quinn, B. T., Dickerson, B. C., Blacker, D., . . . Killiany, R. J. (2006). An automated labeling system for subdividing the human cerebral cortex on MRI scans into gyral based regions of interest. NeuroImage,31(3),968–980. doi:10.1016/j.neuroimage.2006.01.021

[56] Lord, L.-D., Allen, P., Expert, P., Howes, O., Lambiotte, R., McGuire, P., et al. (2011). Characterization of the anterior cingulate's role in the at-risk mental state using graph theory. Neuroimage 56, 1531–1539. doi: 10.1016/j.neuroimage.2011.02.012

[57] Alexander-Bloch, A., Lambiotte, R., Roberts, B., Giedd, J., Gogtay, N., and Bullmore, E. (2012). The discovery of population differences in network community structure: new methods and applications to brain functional networks in schizophrenia. Neuroimage 59, 3889–3900. doi: 10.1016/j.neuroimage.2011.11.035

[58] Alexander-Bloch, A. F., Vértes, P. E., Stidd, R., Lalonde, F., Clasen, L., Rapoport, J., et al. (2013). The anatomical distance of functional

connections predicts brain network topology in health and schizophrenia. Cereb. Cortex 23, 127–138. doi: 10.1093/cercor/bhr388

[59] Caspers, S., Eickhoff, S. B., Zilles, K., & Amunts, K. (2013). Microstructural grey matter parcellation and its relevance for connectome analyses. NeuroImage,80,18–26. doi:10.1016/j.neuroimage.2013.04.003

[60] Papo, D., Zanin, M., & Buldú, J. M. (2014). Reconstructing functional brain networks: Have we got the basics right? Frontiers in Human Neuroscience, 8,107. doi:10.3389/fnhum.2014.00107

[61] Craddock, R. C., James, G. , Holtzheimer, P. E., Hu, X. P. and Mayberg, H. S. (2012), A whole brain fMRI atlas generated via spatially constrained spectral clustering. Hum. Brain Mapp., 33: 1914-1928. doi:10.1002/hbm.21333

[62] Shi J, Malik J. Normalized Cuts and Image Segmentation. IEEE Transactions on Pattern Analysis and Machine Intelligence. 2000;22(8):888–905.

[63] Fan, L., Li, H., Zhuo, J., Zhang, Y., Wang, J., Chen, L., ... Jiang, T. (2016). The Human Brainnetome Atlas: A New Brain Atlas Based on Connectional Architecture. Cerebral Cortex (New York, NY), 26(8), 3508–3526. http://doi.org/10.1093/cercor/bhw157

[64] Desikan RS, Segonne F, Fischl B, Quinn BT, Dickerson BC, Blacker D, Buckner RL, Dale AM, Maguire RP, Hyman BT et al. 2006. An automated labeling system for subdividing the human cerebral cortex on MRI scans into gyral based regions of interest. NeuroImage. 31:968–980.

[65] Behrens TE, Johansen-Berg H, Woolrich MW, Smith SM, Wheeler-Kingshott CA, Boulby PA, et al. Non-invasive mapping of connections between human thalamus and cortex using diffusion imaging, Nat Neurosci , 2003, vol. 6 (pg. 750-7)

[66] Merboldt, K; Hanicke, W; Frahm, J (1985). "Self-diffusion NMR imaging using stimulated echoes". Journal of Magnetic Resonance. 64 (3): 479–486. doi:10.1016/0022-2364(85)90111-8.

[67] Smith et al. 2011: Network modelling methods for FMRI. NeuroImage, 54(2), 875–891

[68] Shannon, C., 1948. A mathematical theory of communication. Bell Syst. Tech. J. 27, 379–423

[69] J. P. W. Pluim, J. B. A. Maintz and M. A. Viergever, "Mutual-information-based registration of medical images: a survey," in IEEE Transactions on Medical Imaging, vol. 22, no. 8, pp. 986-1004, Aug. 2003. doi: 10.1109/TMI.2003.815867

[70] Granger, C.W.J., 1969. Investigating causal relations by econometric models and crossspectral methods. Econometrica 37 (3), 424–438.

[71] Roebroeck, A., Formisano, E., Goebel, R., 2005. Mapping directed influence over the brain using Granger causality and fMRI. Neuroimage 25 (1), 230–242.

[72] Friston, K., 2009. Causal modelling and brain connectivity in functional magnetic resonance imaging. PLoS Biol. 7 (2), e1000033.

[73] Peskin, C. S. (1975). Mathematical aspects of heart physiology. Courant Institute of Mathematical Sciences, New York University, New York.

[74] Dauwels, J., Vialatte, F., Musha, T., Cichocki, A., 2010. A comparative study of synchrony measures for the early diagnosis of Alzheimer's disease based on EEG. Neuroimage 49 (1), 668–693.

[75] Patel, R., Bowman, F., Rilling, J., 2006. A Bayesian approach to determining connectivity of the human brain. Hum. Brain Mapp. 27, 267–276.

[76] Meek, C., 1995. Causal inference and causal explanation with background knowledge. Proceedings of the 11th Annual Conference on Uncertainty in Artificial Intelligence, pp. 403–410.

[77] Korhonen, O., Saarimäki, H., Glerean, E., Sams, M., and Saramäki, J.. Consistency of Regions of Interest as nodes of fMRI functional brain networks. (2017). Network Neuroscience, 1(3), 254-274, doi: 10.1162/NETN_a_00013, November 2017.

[78] Triana Hoyos, A.M. (2018). Effects of spatial smoothing on group-level differences in the structure of functional brain networks (master's thesis). Aalto University School of Science.

[79] Di Martino, A., Yan, C.-G., Li, Q., Denio, E., Castellanos, F. X., Alaerts, K., . . . Milham, M. P. (2014, jun). The Autism Brain Imaging Data Exchange: Towards Large-Scale Evaluation of the Intrinsic Brain Architecture in Autism

[80] Di Martino, A. (2017). Enhancing studies of the connectome in autism using the autism brain imaging data exchange II (Vol. 4). doi: 10.1038/sdata.2017.10

[81] Craddock, C., Benhajali, Y., Chu, C., Chouinard, F., Evans, A., Jakab, A., . . . Bellec, P. (2013). The Neuro Bureau Preprocessing Initiative: open sharing of prepro- cessed neuroimaging data and derivatives. Frontiers in Neuroinformatics(41). Retrieved from http://www.frontiersin.org/neuroinformatics/10.3389/conf.fninf.2013.09.00041/full doi: 10.3389/conf.fninf.2013.09.00041

[82] Faras, H., Al Ateeqi, N., & Tidmarsh, L. (2010). Autism spectrum disorders (Vol. 30) (No. 4). doi: 10.4103/0256-4947.65261

[83] Vasa, R. A., Mostofsky, S. H., & Ewen, J. B. (2016). The Disrupted Connectivity Hypothesis of Autism Spectrum Disorders: Time for the Next Phase in Research. Biological Psychiatry: Cognitive Neuroscience and Neuroimaging, 1(3), 245– 252. Retrieved from http://www.sciencedirect.com/science/article/pii/S2451902216300015 doi: https://doi.org/10.1016/j.bpsc.2016.02.003

[84] Elisa Ryyppä, Enrico Glerean, Elvira Brattico, Jari Saramäki, & Onerva Korhonen 2018. Regions of Interest as nodes of dynamic functional brain networks. Network Neuroscience (in press).https://www.mitpressjournals.org/doi/abs/10.1162/NETN_a_00047.

[85] Magalhães, R., Marques, P., Soares, J., Alves, V., Sousa, N. (2015). The Impact of Normalization and Segmentation on Resting-State Brain Networks. *Brain Connectivity, 5(3),* 166-176.

[86] Andric, M., Hasson, U. (2015). Global features of functional brain networks change with contextual disorder. *NeuroImage, 117,* 103-113

[87] Mossa, S., Barthélémy, Stanley H.E., Nunes Amaral, L.A. (2002). Truncation of Power Law Behavior in "Scale-Free" Network Models due to Information Filtering. Physical Review Letters 88(13), doi: https://doi.org/10.1103/PhysRevLett.88.138701

[88] Jeong, H., Mason S. P., Barabási, A.-L., Oltvai, Z. N. (2011). Lethality and centrality in protein networks. Nature, 411, 41-42.

[89] Newman, M. E. J. (2001). The structure of scientific collaboration networks. PNAS, 98 (2) 404-409. doi: https://doi.org/10.1073/pnas.98.2.404.

[90] Achard, S., Salvador, R., Whitcher, B., Suckling, J., Bullmore, E. (2006). A resilient, low-frequency, small-world human brain functional network with highly connected association cortical hubs. J. Neuroscience, 26(1), 63-72.

[91] Papo D, Zanin M, Martínez JH and Buldú JM (2016) Beware of the Small-World Neuroscientist! Front. Hum. Neurosci. 10:96. doi: 10.3389/fnhum.2016.00096

[92] Ravasz, E. & Barabási, A. L. Hierarchical organization in complex networks. Phys. Rev. E Stat. Nonlin. Soft Matter Phys. 67, 026112 (2003).

[93] Davison EN, Turner BO, Schlesinger KJ, Miller MB, Grafton ST, Bassett DS, et al. (2016) Individual Differences in Dynamic Functional Brain Connectivity across the Human Lifespan. PLoS Comput Biol 12(11): e1005178. doi:10.1371/ journal.pcbi.1005178

[94] Alan C. Evans, Weiqian Dai, D. Louis Collins, Peter Neelin, Sean Marrett, "Warping of a computerized 3-D atlas to match brain image volumes for quantitative neuroanatomical and functional analysis," Proc. SPIE 1445, Medical Imaging V: Image Processing, (1 June 1991); doi: 10.1117/12.45221

[95] Jonas Richiardi, Hamdi Eryilmaz, Sophie Schwartz, Patrik Vuilleumier, Dimitri Van De Ville, Decoding brain states from fMRI connectivity graphs, NeuroImage, Volume 56, Issue 2, 2011, Pages 616-626, ISSN 1053-8119, https://doi.org/10.1016/j.neuroimage.2010.05.081.[93, 94]